Earth-Science Reviews 146 (2015) 163–182

Contents lists available at ScienceDirect

Earth-Science Reviews

journal homepage: www.elsevier.com/locate/earscirev

Surface morphology of fans in the high-Arctic periglacial environment of Svalbard: Controls and processes

Tjalling de Haas [a,*], Maarten G. Kleinhans [a], Patrice E. Carbonneau [b], Lena Rubensdotter [c,d], Ernst Hauber [e]

[a] Faculty of Geosciences, Utrecht University, PO-Box 80115, 3508 TC Utrecht, The Netherlands
[b] Department of Geography, Durham University, DH1 3LE Durham, UK
[c] Department of Arctic Geology, University Centre in Svalbard, Longyearbyen, Norway
[d] Geological Survey of Norway, Trondheim, Norway
[e] Institute of Planetary Research, German Aerospace Center, Rutherfordstrasse 2, DE-12489 Berlin, Germany

ARTICLE INFO

Article history:
Received 31 January 2015
Accepted 6 April 2015
Available online 15 April 2015

Keywords:
Alluvial fan
Colluvial fan
Periglacial
Snow avalanche
Debris flow
Svalbard

ABSTRACT

Fan-shaped landforms occur in all climatic regions on Earth. They have been extensively studied in many of these regions, but there are few studies on fans in periglacial, Arctic and Antarctic regions. Fans in such regions are exposed to many site-specific environmental conditions in addition to their geological and topographic setting: there can be continuous to discontinuous permafrost and snow avalanches and freeze–thaw cycles can be frequent. We study fans in the high-Arctic environment of Svalbard to (1) increase our fundamental knowledge on the morphology and morphometry of fans in periglacial environments, and (2) to identify the specific influence of periglacial conditions on fans in these environments. Snow avalanches have a large geomorphic effect on fans on Svalbard: the morphology of colluvial fans is mainly determined by frequent snow avalanches (e.g., flattened cross-profiles, exposed fine-grained talus on the proximal fan domain, debris horns and tails). As a result, there are only few fans with a rockfall-dominated morphology, in contrast to most other regions on Earth. Slush avalanches contribute significant amounts of sediment to the studied alluvial fans. The inactive surfaces of many alluvial fans are rapidly beveled and leveled by snow avalanches, solifluction and frost weathering. Additionally, periglacial reworking of the fan surface often modifies the original morphology of inactive fan surfaces, for example by the formation of ice-wedge polygons and hummocks. Permafrost lowers the precipitation threshold for debris-flow initiation, but limits debris-flow volumes. Global warming-induced permafrost degradation will likely increase debris-flow activity and -magnitude on fans in periglacial environments. Geomorphic activity on snow avalanche-dominated colluvial fans will probably increase due to future increases in precipitation, but depends locally on climate-induced changes in dominant wind direction.

Contents

* Corresponding author.
E-mail address: t.dehaas@uu.nl (T. de Haas).

http://dx.doi.org/10.1016/j.earscirev.2015.04.004
0012-8252/

1. Introduction

Fan-shaped deposits are conical landforms that commonly develop where a channel emerges from a mountainous catchment to an adjoining valley (Blair and McPherson, 2009). Fans can vary greatly in size and can be roughly divided into (1) colluvial fans (10 s to 100 s m), including talus cones and scree slopes (e.g., Blikra and Nemec, 1998), (2) alluvial fans (100 s m to 10 s km), generally dominated by sediment-gravity flows or fluid-gravity flows (e.g., Blair and McPherson, 2009) and (3) fluvial fans or megafans (>10 s km) (Hartley et al., 2010; Weissmann et al., 2010). These landforms have been described in many environments on Earth (e.g., Blair and McPherson, 2009; Harvey, 2011), Mars (e.g., De Haas et al., 2013; Hauber et al., 2013) and Titan (e.g., Lorenz et al., 2008). Terrestrial regions wherein fans are present include arid to semi-arid regions (e.g., Whipple and Dunne, 1992; Al-Farraj and Harvey, 2000; Hartley et al., 2005), humid temperate regions (e.g., Moscariello et al., 2002; Saito and Oguchi, 2005; Chiverrell et al., 2007), Alpine environments (e.g., Kostaschuk et al., 1986; Derbyshire and Owen, 1990; Cavalli et al., 2008), the humid tropics (e.g., Kesel and Spicer, 1985) and periglacial, Arctic and Antarctic environments (hereafter termed 'periglacial') (e.g., Catto, 1993; Webb and Fielding, 1999; Davies et al., 2003). While especially fans in arid to semi-arid, Alpine and temperate environments have been extensively studied, fans in periglacial environments have received little attention.

The influence of climate on fan formation has long been under debate; some authors believe that changes in climate will be preserved as differences in fan facies and morphology (e.g., Nemec and Postma, 1993; Dorn, 1994; Ritter et al., 1995), whereas others suggest that climate is rarely the main factor governing fan characteristics (e.g., Blair and McPherson, 1994, 2009). Many different studies suggest that processes leading to fan deposits differ little between humid and arid environments, or between Arctic and subtropical environments (e.g., Brierley et al., 1993; Ibbeken et al., 1998; Krzyszkowski and Zieliński, 2002; Harvey et al., 2005; Lafortune et al., 2006), and accordingly fans and debris flows in periglacial regions were found to be not significantly distinct from those in other climates (Catto, 1993; Harris and Gustafson, 1993; Webb and Fielding, 1999). However, fans in periglacial environments are subject to different environmental conditions compared to fans in other climate zones; there can be continuous or discontinuous permafrost, precipitation occurs generally dominantly as snow, snow avalanches can be frequent in mountainous regions and freeze–thaw cycles occur regularly leading to pervasive weathering (e.g., Matsuoka, 1991; Eckerstorfer and Christiansen, 2011a, 2011b). As temperatures are below the freezing point for the largest part of the year, most geomorphic activity is typically limited to a narrow window in the spring and summer months when snow and ice are able to melt and precipitation is able to occur as rain. Recently deglaciated periglacial environments expose landscapes that are in an unstable state, and consequently liable to rapid modification, erosion and sediment release at rates greatly exceeding background denudation rates (e.g., Brazier et al., 1988; Eyles and Kocsis, 1988; Ballantyne, 2002; Mercier et al., 2009). Such accelerated geomorphic activity after deglaciation is termed 'paraglacial' (e.g., Ryder, 1971; Ballantyne, 2002). These different controls raise the question to what degree fan formation, deposits and morphology in periglacial environments differ from those in other environments. This is largely unknown due to the small number of studies on periglacial fans (Legget et al., 1966; Catto, 1993; Harris and McDermid, 1998; Webb and Fielding, 1999), illustrating the need for detailed descriptions of fans in these environments.

The ongoing global atmospheric warming especially affects the polar and periglacial regions (e.g., Christiansen et al., 2010; Førland et al., 2012). Mainly, it leads to extensive glacier and permafrost degradation (e.g., Benestad, 2005; Etzelmüller et al., 2011), thereby increasing slope activity and hazard potential (e.g., Harris et al., 2011). As fluvial- and alluvial fans are preferred sites for settlements (e.g., Cavalli et al., 2008), this emphasizes the need for a detailed understanding of fans in periglacial environments. For example, catastrophic slope processes, including debris flows and snow avalanches, claimed numerous lives and had considerable economic effects during the last century in periglacial regions such as Iceland, Norway and Svalbard (Jahn, 1967; Jóhannesson and Arnalds, 2001; Decaulne and Sæmundsson, 2003, 2007; Nesje et al., 2007).

Here we aim to (1) increase our fundamental knowledge on the morphology and morphometry of fans in periglacial environments and to (2) identify the influence of periglacial conditions, such as snow avalanches and continuous permafrost, on fan formation, morphology and morphometry, by studying colluvial and alluvial fans on Svalbard.

In addition to a literature review on slope processes in the periglacial environment of Svalbard, which are responsible for the transport to and redistribution of sediment on fans, a large number of colluvial and alluvial fans were studied in the Adventdalen region on the island of Spitsbergen, in the vicinity of Svalbard's capital Longyearbyen (Fig. 1; Table 1; Figs. S1–S6). This region was chosen for its high-Arctic location and excellent field research infrastructure including availability of high-resolution imagery and topographic data. Moreover, there have been numerous studies on slope processes on Svalbard (e.g., Rapp, 1960; Jahn, 1967; Bibus, 1975; Larsson, 1982; Åkerman, 1984; André, 1990a, 1990b; Siewert et al., 2012; Eckerstorfer et al., 2013), enabling detailed understanding of the processes involved in fan formation.

This paper is organized as follows. First, data and methods are described. Next, a detailed summary of the climate, geology and geomorphic slope processes on Svalbard is given, as these factors together are responsible for the formation and characteristics of the fans. Then, the morphology and morphometry of the studied fans in the Adventdalen region are described, in order to identify characteristics that can be unique for fans in periglacial environments. Finally, the specific characteristics that differentiate periglacial fans from those in other environments are discussed, followed by a brief discussion on the effect of present global warming and associated natural hazards on fans in periglacial environments.

2. Data and methods

This study is based on a combination of high-resolution imagery and geomorphological fieldwork. High-resolution imagery was acquired

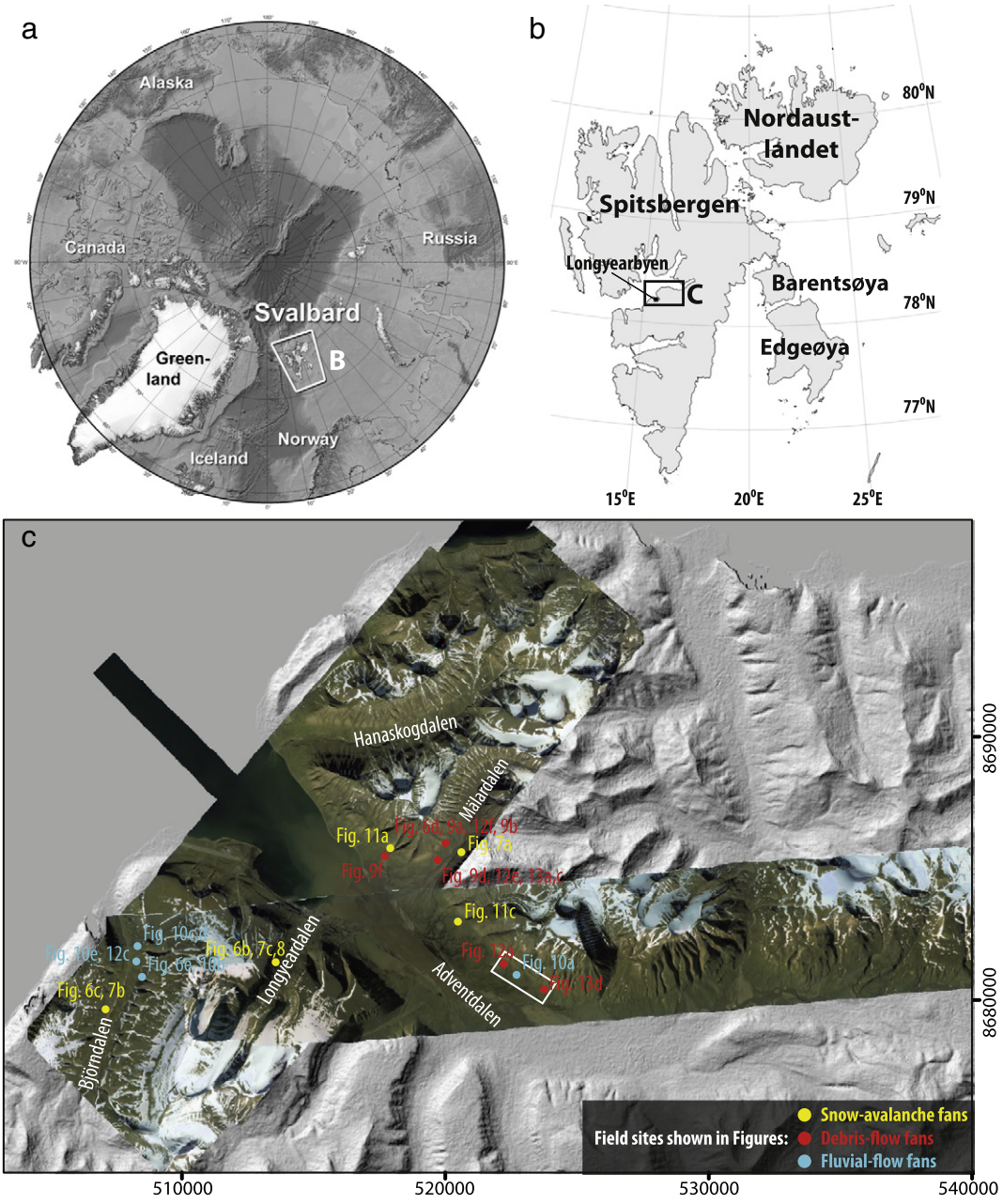

Fig. 1. Context maps of the study area. (a) Map of the Arctic, with location of Svalbard highlighted. (b) Map of Svalbard showing the study area. (c) Study area (Adventdalen region), with locations of field sites and figures shown in this paper indicated. Base image: HRSC-AX image mosaic (approximately true color) on top of hillshaded version of ASTER DEM. White outline in Adventdalen indicates extent of UAV imagery. Coordinates in UTM WGS84 33N.
Image modified from Hauber et al. (2011).

during a flight campaign in the summer of 2008 with the airborne high resolution stereo camera (HRSC-AX) (Gwinner et al., 2000; Neukum and the HRSC-Team, 2001) and a flight campaign in the summer of 2009 with an unmanned airborne vehicle (UAV) carrying a Pentax Optio A4 camera.

The HRSC-AX is a digital pushbroom (linear array charge-coupled device [CCD]) scanner with nine channels for nadir panchromatic, stereo panchromatic and color imaging, similar to its planetary counterpart HRSC on the *Mars Express* (Jaumann et al., 2007). The images cover ~450 km^2 in the Adventdalen region, large parts of Adventdalen, Bjørndalen, Longyeardalen, Hanaskogdalen and Mälardalen (Fig. 1c). The processed color and panchromatic nadir ortho-images have a spatial resolution (i.e., ground sampling distance) of 20 cm, while the digital elevation models (DEMs) derived from stereo images have a spatial resolution of 50 cm.

The UAV images were acquired by Kolibri Geo Services. In total 165 images were shot covering multiple fan systems in Adventdalen, which we processed with Agisoft Photoscan software (Agisoft, 2011) into a georeferenced orthorectified image with a spatial resolution of 7 cm/px. Agisoft Photoscan uses structure from motion in a photogrammetric workflow with high levels of automation and good levels of data quality (Fonstad et al., 2013), see De Haas et al. (2014) for details on its application to the alluvial fan environment.

A surface particle-size map was made of multiple colluvial fans with the HRSC-AX images and ground truthing via photosieving, based on the methods of Carbonneau et al. (2004) and Carbonneau (2005), in

Table 1
Geomorphic data of the studied alluvial fans. Fan type abbreviations: AF = cone-shaped snow avalanche-dominated colluvial fan, AFt = tongue-shaped snow avalanche-dominated colluvial fan, DF = debris-flow-dominated fan, FF = fluvial-flow-dominated fan. Note that these abbreviations are based on the processes that dominate the surface morphology of the fans, and do not necessarily refer to the dominant mechanism of aggradation (some of the colluvial fans have a snow avalanche-dominated surface but might have been mainly aggraded by rock falls). Apex coordinates in UTM WGS84 33N. See Supplementary materials for orthophotos of all the fans shown in this table.

No	Valley	Fan type	Apex X	Apex Y	Catchment area, m^2	Catchment relief, m	Catchment length, m	Catchment slope, °	Fan area, m^2	Fan relief, m	Fan length, m	Fan slope, °
1	Longyeardalen	AFt	512,423	8,680,605	16,098	172	223	38	17,621	149	266	29
2	Longyeardalen	AF	512,496	8,680,678	16,469	162	210	38	22,165	165	263	32
3	Longyeardalen	AF	512,939	8,681,249	29,512	235	268	41	15,354	110	232	25
4	Longyeardalen	AF	512,991	8,681,393	37,922	230	280	39	20,407	122	221	29
5	Longyeardalen	AF	513,024	8,681,498	22,008	225	264	40	12,026	128	228	29
6	Longyeardalen	AF	513,056	8,681,591	27,333	226	277	39	16,719	132	242	29
7	Longyeardalen	AF	513,095	8,681,672	28,800	230	296	38	17,465	126	241	28
8	Longyeardalen	AF	513,131	8,681,758	22,213	221	271	39	20,512	140	280	27
9	Longyeardalen	AF	513,185	8,681,867	21,026	225	288	38	14,038	126	246	27
10	Longyeardalen	AF	513,215	8,681,954	28,646	203	259	38	17,036	135	255	28
11	Longyeardalen	AF	513,254	8,682,029	17,953	198	259	37	15,013	173	299	30
12	Longyeardalen	AF	513,313	8,682,097	28,562	207	274	37	16,414	156	286	29
13	Longyeardalen	AF	513,768	8,680,667	18,913	174	188	43	18,250	155	335	25
14	Longyeardalen	AF	513,789	8,680,780	23,617	206	241	40	25,744	139	336	23
15	Longyeardalen	AF	513,856	8,680,905	29,478	205	252	39	21,757	139	311	24
16	Longyeardalen	AF	513,922	8,680,987	18,850	194	233	40	25,526	161	378	23
17	Longyeardalen	AF	513,926	8,681,064	15,292	214	260	39	21,806	135	301	24
18	Hanaskogdalen	DF	515,638	8,690,657	230,571	357	867	22	73,043	75	420	10
19	Hanaskogdalen	DF	516,130	8,690,708	356,622	522	1074	26	198,763	101	597	10
20	Hanaskogdalen	DF	516,374	8,690,662	139,670	501	915	29	123,802	97	519	11
21	Hanaskogdalen	DF	516,695	8,690,688	172,311	620	999	32	167,826	113	571	11
22	Hanaskogdalen	DF	517,326	8,690,662	250,361	606	1124	28	341,782	110	727	9
23	Hanaskogdalen	DF	517,999	8,690,788	335,505	477	1076	24	184,029	93	527	10
24	Hanaskogdalen	DF	518,329	8,690,854	193,885	446	1035	23	78,200	76	464	9
25	Hanaskogdalen	DF	518,561	8,690,930	370,714	555	1207	25	137,003	80	487	9
26	Hanaskogdalen	DF	519,013	8,691,190	283,326	588	1128	28	270,715	98	595	9
27	Hanaskogdalen	DF	519,579	8,691,578	279,051	626	1157	28	269,162	115	579	11
28	Hanaskogdalen	DF	520,070	8,691,806	307,707	555	1182	25	215,805	87	544	9
29	Hanaskogdalen	DF	520,311	8,691,885	231,832	513	1246	22	92,487	67	434	9
30	Mälardalen	DF	519,264	8,685,816	275,167	511	1024	27	222,839	87	462	11
31	Mälardalen	DF	519,639	8,686,280	226,492	516	938	29	246,719	96	513	11
32	Mälardalen	AFt	520,569	8,685,626	–	–	–	–	60,410	127	463	15
33	Adventdalen	FF	516,744	8,686,209	2,254,686	830	2355	19	403,853	80	619	7
34	Adventdalen	DF	517,599	8,685,897	869,820	784	1776	24	231,037	108	696	9
35	Adventdalen	DF	518,268	8,685,449	435,373	555	1372	22	210,850	96	661	8
36	Adventdalen	DF	521,910	8,681,768	–	–	–	–	21,757	23	172	8
37	Adventdalen	DF	522,142	8,681,598	–	–	–	–	63,640	41	306	8
38	Adventdalen	FF	522,693	8,681,222	–	–	–	–	77,040	48	301	9
39	Adventdalen	FF	523,250	8,680,851	749,548	804	1934	23	106,164	42	257	9
40	Adventdalen	DF	523,716	8,680,690	220,045	576	1360	23	125,966	66	483	8
41	Bjørndalen	AF	506,941	8,681,423	15,831	150	192	38	19,060	146	222	33
42	Bjørndalen	AF	506,948	8,681,527	7833	147	178	40	11,366	158	233	34
43	Bjørndalen	AF	506,959	8,681,588	12,104	161	197	39	16,569	157	243	33
44	Bjørndalen	AF	506,955	8,681,675	19,851	165	217	37	26,098	161	260	32
45	Bjørndalen	AF	506,945	8,681,768	16,572	172	222	38	15,941	161	259	32
46	Bjørndalen	AF	506,936	8,681,860	18,576	179	231	38	20,656	162	289	29
47	Bjørndalen	AF	506,940	8,681,949	20,045	190	248	38	26,156	150	261	30
48	Bjørndalen	AF	506,888	8,682,067	17,737	166	209	38	23,045	176	272	33
49	Bjørndalen	AF	506,839	8,682,196	23,636	159	196	39	29,270	183	290	32
50	Bjørndalen	AF	506,795	8,682,365	20,518	170	214	38	27,415	169	281	31
51	Bjørndalen	AF	506,767	8,682,436	7489	148	163	42	12,946	157	242	33
52	Bjørndalen	AF	506,732	8,682,509	28,425	172	235	36	28,807	172	304	29
53	Bjørndalen	AFt	506,643	8,680,132	16,805	183	291	32	14,151	97	228	23
54	Bjørndalen	DF	506,899	8,681,200	194,619	247	930	15	59,915	117	334	19
55	Bjørndalen	FF	508,166	8,682,505	1,467,265	295	2239	8	165,526	147	673	12
56	Bjørndalen	FF	508,081	8,682,022	1,520,048	369	2808	7	246,883	81	612	8
57	Bjørndalen	FF	508,034	8,681,459	591,600	305	1832	9	126,142	97	494	11
58	Bjørndalen	FF	507,939	8,681,036	637,795	344	1809	11	133,935	88	488	10
59	Bjørndalen	FF	507,689	8,680,637	834,094	325	1709	11	178,898	61	543	6
60	Bjørndalen	FF	507,449	8,680,089	612,757	383	1642	13	151,291	74	481	9
61	Bjørndalen	FF	507,209	8,679,662	297,860	323	1558	12	102,553	61	417	8
62	Bjørndalen	FF	507,113	8,679,433	344,199	367	1629	13	119,680	60	415	8

which image texture (i.e., entropy) is correlated to the median size of the particles. This approach relies on variations of brightness values induced by surface particles. Larger particles cast larger, but localized, shadows thus leading to more variation and light/dark contrasts. This method requires an empirical calibration for each image data set. For a detailed description on the procedures for photosieving and application of this method to the alluvial fan environment the reader is referred to De Haas et al. (2014). Calibration results of HRSC-AX image entropy and median particle size are given in Fig. 2.

Morphometric analyses of fans and catchments were performed in ArcMap 10. Fan and catchment area were visually delineated from the aerial images and DEM. Catchment relief was defined as the elevation

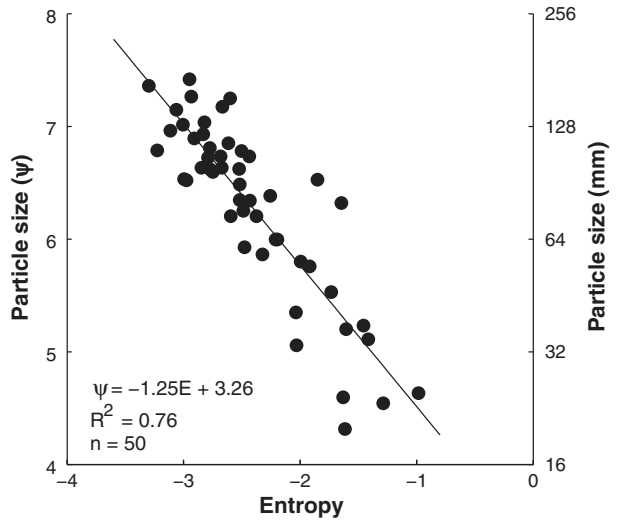

Fig. 2. Empirical relation between image entropy in the HRSC-AX image and arithmetic median particle size derived from photosieving. Locations were matched by DGPS and context images.

difference between the highest point of the catchment and the fan apex. Catchment length and slope were measured over a straight line connecting the highest point in the catchment with the fan apex. Fan relief was defined as the elevation difference between the fan apex and the lowest point at the fan toe. Fan length and slope were measured over a straight line connecting these two points.

We conducted field site visits for geomorphological observations on fans in Adventdalen, Bjørndalen, Longyeardalen, Hanaskogdalen and Mälardalen in August 2013 (Fig. 1). Processes responsible for the fan morphology were identified by conventional field reconnaissance (cf. Blair and McPherson, 1994; Blikra and Nemec, 1998). The summer season of 2013 was relatively wet, with a total amount of precipitation of 123 mm at Svalbard airport, compared to 25 mm in 2011 and 50 mm in 2012. Hence, there was a relatively large amount of vegetation at the surface, and debris flows occurred on a few fans in our study area during the fieldwork period, providing a detailed insight into their formative processes and composition.

3. Svalbard climate, geology and geomorphic processes

3.1. Geological and climatic setting

The present climate of Svalbard is arctic with mean annual temperatures ranging between −6 °C at sea level and −15 °C in the high mountains. In the Adventdalen area the coldest (February) and warmest (July) months have mean temperatures of −15.2 °C and 6.2 °C, respectively, and the mean annual air temperature is −5.8 °C (Hanssen-Bauer and Førland, 1998). Yearly average precipitation is low and reaches ~180 mm in central Spitsbergen, whereas along the coast of Svalbard precipitation ranges between 400 and 600 mm. Snow is the dominant precipitation type: around 75% of the precipitation events are snow at Longyearbyen airport (Førland and Hanssen-Bauer, 2003). Interannual differences in mean precipitation and temperatures can be high. Heavy snowfalls generally occur in December and January, and snow avalanches are frequent, especially on downwind slopes (Vogel et al., 2012). Mean annual temperatures have increased by ~1 °C per decade during the last decades on Svalbard, while winter warming is even more dramatic, with an increase of 2–3 °C per decade. Mean annual precipitation has increased with 2–4% per decade (Førland et al., 2012). On average, the Adventdalen area has 5–14 days a month with winds stronger than 14 m s^{-1} and up to 5 days with winds exceeding 25 m s^{-1} (Førland et al., 1997). The strongest winds predominate in winter, and therefore snowpacks thicker than 1 m accumulate only in local wind shadows. Local wind shadows are mainly ravines, stream channels and cornices, which are wedge-like snowdrifts that form on lee sides of ridges and slope inflections (Latham and Montagne, 1970; Eckerstorfer et al., 2012; Vogel et al., 2012). About 60% of Svalbard is covered by glaciers and ice caps, whereas the remainder is characterized by continuous permafrost (Brown et al., 1997). Surficial runoff of meltwater is limited to two or three summer months, when it is accompanied by scarce rainfall (Lønne and Nemec, 2004). Permafrost thickness is 10–40 m in coastal regions and ~100 m in major valleys, but can increase to more than 450 m in the highlands (Liestøl, 1976; Sollid et al., 2000; Isaksen et al., 2001). The active layer of the permafrost, the layer that annually thaws in summer and is available for erosion, has a thickness of 0.4–1 m depending on topography (Åkerman, 1984; Christiansen et al., 2010; Harris et al., 2011). Permafrost surface temperatures have increased by 0.5–2 °C in the last century (Isaksen et al., 2000; Etzelmüller et al., 2011), and the present decadal warming rate at the permafrost surface is in the order of 0.07 °C yr^{-1}, with indications of accelerated warming in the last decades (Isaksen et al., 2007). As a result, active-layer thickness has increased over the last decades (Åkerman, 2005; Etzelmüller et al., 2011).

The Adventdalen region is dominated by an extensive plateau mountain massif, rising to an average elevation of 450–550 m above sea level (a.s.l.). The highest peaks in the area reach up to 1000 m a.s.l and have an Alpine topography. The plateau mountains are separated by glacio-fluvially eroded U-shaped valleys that deglaciated around 10,000 yr BP (Mangerud et al., 1992; Svendsen and Mangerud, 1997), causing widespread paraglacial activity (André, 2003; Lønne and Nemec, 2004; Mercier et al., 2009; Rachlewicz, 2010). Geologically, the bedrock of the massifs bordering Adventdalen consists of Jurassic and Cretaceous sediments that belong to the Helvetiafjellet and Carolinefjellet Formations (Dallmann et al., 2001, 2002). These formations are characterized by subhorizontal layers (centimeters to tens of centimeters) of sandstones, siltstones, shales and some thin coal seams (Parker, 1967; Major and Nagy, 1972). Bedrock weathering is driven mainly by frost (Lønne and Nemec, 2004), producing large amounts of weathered material, including abundant clays (Jahn, 1976; Sørbel et al., 2011). The short distance from the high mountains to the ocean causes strong downstream grain-size fining (Frings, 2008) from the fans into the large rivers and fan deltas in the fjords. In the Adventdalen region loess (Bryant, 1982) and Arctic meadow (Van Vliet-Lanoë, 1998) soils are present, characterized by a high organic content. The low-sloping parts of the region are covered by a moist open tundra vegetation, including mosses, grasses and herbs and few dwarf shrubs (Rozema et al., 2006). Long-inactive parts of alluvial fans are often vegetated. The steeper and geomorphologically more active colluvial fans are largely unvegetated.

3.2. Review of geomorphic processes on the periglacial slopes of Svalbard

Slopes on Svalbard are mainly modified by a combination of rockfalls, snow avalanches, debris flows, fluvial flows (i.e. stream flows and hyperconcentrated flows) and various slow mass-wasting processes, of which solifluction is the most important (e.g., Rapp, 1960; Jahn, 1967; Larsson, 1982; Åkerman, 1984; André, 1990a, 1990b; Lønne and Nemec, 2004; Siewert et al., 2012; Eckerstorfer et al., 2013). Principal sources of flowing water are the melting of snow, glaciers and the thawing of the active layer, combined with rain showers (e.g., Lønne and Nemec, 2004). These slope processes determine the water and sediment fluxes onto the fans and are therefore briefly reviewed in this section. We especially focus on snow avalanches, as these are common in periglacial and Alpine environments and therefore generally overlooked in current alluvial-fan research.

3.2.1. Snow avalanches

Snow avalanches are very frequent on Svalbard and numerous snow avalanches are triggered on a yearly basis in the Adventdalen region (e.g., Eckerstorfer and Christiansen, 2011a, 2011b). The main types of snow avalanches are cornice-fall avalanches, slab avalanches, loose snow avalanches and slush avalanches (Eckerstorfer and Christiansen, 2011b).

Most snow avalanches in the Adventdalen region are cornice-fall avalanches from cornices that accumulated along plateau edges (45%) (Eckerstorfer and Christiansen, 2011b). Cornice accumulation is caused by strong and continuous wind activity on the widespread plateau mountains, which causes transport of snow across the plateaus. Cornices are today most frequent on W–NW oriented slopes because of the prevailing regional SE wind direction in the snow season (Eckerstorfer and Christiansen, 2011b; Vogel et al., 2012). Consequently, snow-avalanche-induced sediment accretion rates on NW facing slopes are more than twice as high as on SE facing slopes (Vogel et al., 2012; Eckerstorfer et al., 2013). Cornice-fall avalanches generally occur on a yearly basis below many plateau edges (Eckerstorfer and Christiansen, 2011b; Eckerstorfer et al., 2013). They mainly take place at the end of the snow season around June, when tension cracks develop and grow between the cornice mass and the plateau (Vogel et al., 2012). Cornices are thus able to significantly erode the plateau edge and rockwall during their formation (a process termed 'cornice plucking'; Vogel et al., 2012; Eckerstorfer et al., 2013).

Slab avalanches are the second most dominant, and generally largest, snow avalanche type (32%), releasing equally on all slope aspects (Eckerstorfer and Christiansen, 2011b). These avalanches result from failure in a weak layer or interface, generally consisting of a thin layer of hoar formed by condensation of water vapor (e.g., Jamieson and Schweizer, 2000), underlying a cohesive slab layer. They are mainly triggered by additional snow loading as well as distinctive cooling or warming of the upper snow layers (Eckerstorfer and Christiansen, 2011b).

Loose snow avalanches (22% of recorded snow avalanches) often result from failure of snow that has been deposited at a steeper angle than the natural angle of repose of snow, typically ~30° (Blikra and Nemec, 1998; Eckerstorfer and Christiansen, 2011b). They usually start at a point or small area and expand as they move, implying that more snow is entrained in the process and that the presence of loose snow is a necessary condition. The majority of loose snow avalanches occur at the end of the snow season, releasing mainly on south facing slopes due to the higher direct solar radiation (Eckerstorfer and Christiansen, 2011b).

Slush avalanches only comprise a minor percentage of the total amount of snow avalanches (1%), but do occur on a yearly basis in the Adventdalen region (Eckerstorfer and Christiansen, 2011b, 2012). Slush avalanches typically occur in Arctic regions. They are triggered by an increase in the content of free water in the snowpack which decreases snowpack strength (Nyberg, 1989). The free water increase can be caused by intensive spring melting of snow and/or rain on snow events (e.g., Jahn, 1967; André, 1995; Hestnes, 1998; Decaulne and Sæmundsson, 2006), and is exacerbated by an impermeable permafrost table that acts as an aquiclude. In contrast to dry snow avalanches, wet slush avalanches can be generated on slopes as low as 10° (Blikra and Nemec, 1998). The vast majority of slush avalanches move through narrow gorges, where snow accumulates and persists longer into the melting season, and flow out onto alluvial fans (Eckerstorfer and Christiansen, 2012).

Snow avalanches can have a considerable geomorphic effect if they are able to erode sediment (e.g., Luckman, 1977; Åkerman, 1984; Nyberg, 1989; André, 1990a, 1990b; Blikra and Nemec, 1998; Decaulne and Sæmundsson, 2006; Eckerstorfer et al., 2013; Laute and Beylich, 2014). However, only a limited subset of all snow avalanches accomplish significant sediment transport: most snow avalanches only redistribute the surface snow cover without coming into contact with the underlying ground surface. Avalanche erosion only occurs when avalanches run over bare ground or involve the full depth of the snow cover (e.g., Luckman, 1977). Vegetation cover may also protect the underlying surface from erosion. Hence, the erosion potential of avalanches is highest on loose, unconsolidated debris mantles covered by no or a limited amount of snow (Luckman, 1977). Therefore, cornice fall and slush avalanches have the largest geomorphic effect (André, 1990a, 1990b; Eckerstorfer et al., 2013), as they regularly occur at the end of the snow season from retained snow accumulations at the top of slopes and in couloirs, ravines and gullies, while their surroundings are free of snow or covered by a thin layer of snow only.

Important morphological indicators for snow avalanche erosion and sedimentation are perched or balanced cobbles and boulders, which came to rest on top of each other after melting of the snow avalanches (Rapp, 1960; Luckman, 1977, 1992; Decaulne and Sæmundsson, 2006), arcuate accumulations of debris, bulldozed ahead by avalanches marking the base of the avalanche track (Rapp, 1960; Luckman, 1977; Jomelli and Francou, 2000), debris tails, tails of debris that are present in the lee of large immobile obstacles, generally cobbles or boulders, where erosion is prevented (Blikra and Nemec, 1998) and debris horns, accumulated sediment on the upslope side of immobile obstacles due to local plastic freezing of avalanches rich in sediment (Blikra and Nemec, 1998). Moreover, steep mountain walls of snow avalanche-dominated upper catchments are often dissected by narrow parallel or funnel shaped avalanche chutes, which are rounded valleys with an open, flat-bottomed, U-shaped cross profile that formed by pervasive avalanche erosion (e.g., Rapp, 1960; Luckman, 1977).

3.2.2. Rockfall

Rockfall, the downward falling, rolling or skipping of rock fragments under the force of gravity, is a common process on Svalbard. Bedrock on Svalbard is mainly exposed to frost weathering (e.g., Matsuoka, 1991), thereby releasing rock from cliff faces and delivering considerable amounts of sediment to talus slopes or, if funneled, colluvial fans (e.g., Rapp, 1960; Jahn, 1967, 1976; Larsson, 1982; Åkerman, 1984; André, 1986, 1990b, 1997; Siewert et al., 2012). Rockwall weathering and erosion rates mainly depend on rockwall lithology, aspect, elevation and erosional processes. Due to the weak to moderate rock mass strength of the sedimentary sandstones, siltstones and shales in the Adventdalen region, rockwall weathering rates and rockfalls are among the highest on Svalbard and other Arctic regions (Siewert et al., 2012). Sediments are eroded by a combination of frost-weathering and subsequent rockfall (Siewert et al., 2012; Eckerstorfer et al., 2013), cornice plucking (Vogel et al., 2012) and rockwall erosion by avalanches (Humlum et al., 2007; Siewert et al., 2012; Eckerstorfer et al., 2013). Rockwall retreat rates on Svalbard significantly decreased after an initial paraglacial increase since deglaciation (André, 1997, 2003), and colluvial fan accumulation rates decreased accordingly. However, on steep northwest-facing slopes where large snow cornices develop rockwall retreat rates remain similar to early paraglacial retreat rates, due to the present intensive erosion by cornice-fall avalanches (Vogel et al., 2012; Eckerstorfer et al., 2013).

3.2.3. Debris flows

Debris flows are abundant on steep slopes on Svalbard. Bedrock weathering in the Adventdalen region, mainly comprising sedimentary sandstones, siltstones and shales, yields a wide range of sediments including many fines (i.e., silt and clay), which is ideal for the formation of debris flows in combination with the steep hillslopes and permafrost ground (e.g., Blair, 1999; Harvey, 2010). The debris flows in this region are mainly triggered by heavy rainstorms in summer (Thiedig and Kresling, 1973; Bibus, 1975; Larsson, 1982; Rapp, 1985), but rapid snowmelt has also triggered large debris flows in a few known cases (Rapp, 1986). Permafrost slopes, especially in Arctic fine-grained soils (Harris and Lewkowicz, 2000; Lewkowicz and Harris, 2005), are prone to slips and slides. This is caused by the permafrost table which acts as

an aquiclude and a potential failure plane during periods of elevated pore pressure (i.e. active-layer detachment), after summer rainfall events or extreme thaw periods (e.g., Larsson, 1982; Sattler et al., 2011). The co-existence of frozen and unfrozen moisture in soil-voids close to the seasonally shifting thawing plane increases the probability of active-layer failure (Nater et al., 2008). In these permafrost conditions, rainfall intensities as low as 2.5 mm/h can cause debris flows (Larsson, 1982), which is a much lower threshold than in other climatic regions (Caine, 1980). André (1990a) found that debris flows on Svalbard are relatively small-sized because off the limited active-layer depth (0.4–1 m; Åkerman, 1984; Christiansen et al., 2010). Such a limited active-layer depth restricts debris-flow volume by limiting the volume of debris available for remobilization. The largest debris flows are most likely to occur in mid to late summer, when the active-layer depth is at its maximum and shear forces on the slopes are close to the threshold for failure, especially after periods of longlasting rain. For example, 30.8 mm precipitation during a 12 h period between 10 and 11 July 1972 triggered many debris flows in the Adventdalen region (Jahn, 1967; Thiedig and Kresling, 1973; Larsson, 1982). However, these catastrophic events occur rarely on Svalbard due to the infrequent occurrence of heavy rainfalls (André, 1990a, 1995; Reiss et al., 2011). Debris-flow return periods were tentatively estimated from lichenometry at 80 to 500 years in northwestern and central Svalbard (André, 1990a, 1995), but are probably higher on most of the studied fans in the Adventdalen region, given the pristine morphology and lack of lichen and vegetation on many debris-flow deposits.

3.2.4. Fluvial flows: stream and hyperconcentrated flows

Fluvial flows appear to only have a minor geomorphic effect on steep slopes on Svalbard. However, small incised channels on talus slopes and fans continuously convey small amounts of discharge from snowmelt in spring and summer. Snow patches survive until late summer in sheltered depressions like gully-head alcoves. Even in late summer, these snow patches feed small streams within gullies and fans (Reiss et al., 2011). Additionally, fluvial flow from higher parts of the slopes can load remnant snow patches with excess water, potentially inducing slush avalanches. During snowmelt drainage is often concentrated on the slope surface due to the shallow active-layer depth, testified by many rills on the slopes (Larsson, 1982). Fluvial flows mainly have a significant geomorphic importance on fans with relatively large and low sloping catchments as well as valley bottoms (e.g., Bogen and Bønsnes, 2003; Lønne and Nemec, 2004; Szpikowski et al., 2014), where relatively large amounts of water are able to concentrate. Paraglacial activity (Lønne and Nemec, 2004; Mercier et al., 2009; Rachlewicz, 2010) following the last major deglaciation has caused extensive fanhead incision on many fluvial fans on Svalbard (Lønne and Nemec, 2004). These fans are fed by large catchments, where cirque glaciers were generally present during glacial periods. After retreat of these glaciers, large amounts of sediment were ready for transport and fan construction, but when sediment supply from the catchments ceased, fan aggradation rates decreased accordingly, leading to the large fan incisions (Lønne and Nemec, 2004).

3.2.5. Slow mass-wasting

Solifluction is the dominant form of slow mass wasting on Svalbard (e.g., Åkerman, 1984; Harris et al., 2011). It depends on seasonal frost heave, thaw consolidation of the active layer and snowmelt and rainfall in summer, resulting in saturation and movement of the upper surface soil layer (Matsuoka, 2001; Harris et al., 2011). Solifluction landforms are widespread on Svalbard, and include extensive solifluction sheets, sorted and non-sorted solifluction lobes, stripes and steps or terraces, hummocks and talus creep (e.g., Jahn, 1967; Åkerman, 1984; Matsuoka and Hirakawa, 2000; Sørbel and Tolgensbakk, 2002; Åkerman, 2005; Harris et al., 2011; Johnsson et al., 2012). Movement of solifluction lobes and sheets ranges between 2 and 5 cm yr^{-1} across Svalbard (Jahn, 1976; Matsuoka and Hirakawa, 2000; Sørbel and Tolgensbakk, 2002; Åkerman, 2005; Harris et al., 2011), whereas movement outside solifluction lobes is lower and generally does not exceed 0.7 cm yr^{-1} (Sørbel and Tolgensbakk, 2002). Solifluction rates are highest on steep talus slopes; at Kapp Linné talus creep caused an average surface displacement of 8.9 cm yr^{-1} between 1972 and 2002 (Åkerman, 2005).

3.2.6. Relative effectiveness of slope processes

The slope processes reviewed above rarely act in isolation and the dominant geomorphic processes differ from one slope or catchment to the other, depending among others on lithology, meteorology, slope and aspect. On many slopes solifluction is the dominating mass-wasting process on a year-to-year basis (Matsuoka, 2001; Åkerman, 2005), while episodic and rapid processes (e.g., debris flows and snow avalanches) are much more important in terms of total long-term mass movement (Åkerman, 2005). Although the transported amount of sediment per dry snow avalanche is generally much lower than per debris flow, fluvial flow or slush avalanche, the much higher frequency of cornice avalanches on steep slopes below the plateau mountains results in a larger geomorphic effect of cornice avalanches on most of these slopes (Eckerstorfer et al., 2013). This suggests that rockfall and snow avalanches are important sediment transport mechanisms on Svalbard fans below steep catchments and rockwalls, whereas debris flows, fluvial flows and slush avalanches are more abundant on fans below lower sloping catchments.

4. Observations on morphology and morphometry of fans on Svalbard

Three main types of fans were distinguished in the study region: (1) colluvial fans mainly formed by snow avalanches and additional rock falls, but with a snow avalanche-dominated morphology (AF and AFt), (2) alluvial fans dominantly formed by debris flows (DF) and (3) alluvial fans dominantly formed by fluvial flows (FF) (Figs. 3 and 4; Table 1; Figs. S1–S6). Below the morphology and morphometry of these fan types are described to identify the various contributions of the slope processes described above to fan formation and to identify the effect of periglacial (snow- and permafrost-related) processes on these fans.

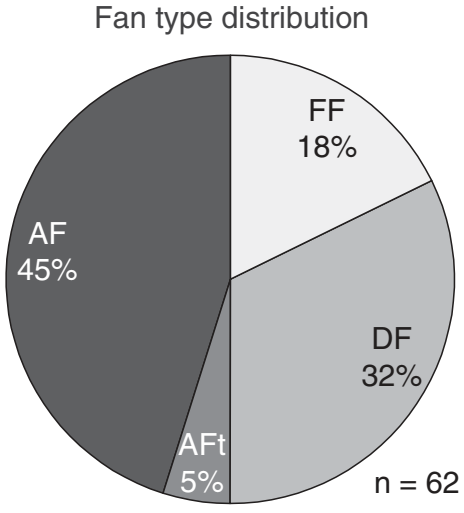

Fig. 3. Breakdown of fans by dominant formative mechanism (Table 1). Fan type abbreviations: AF = cone-shaped snow avalanche-dominated colluvial fan, AFt = tongue-shaped snow avalanche-dominated colluvial fan, DF = debris-flow-dominated fan, and FF = fluvial-flow-dominated fan.

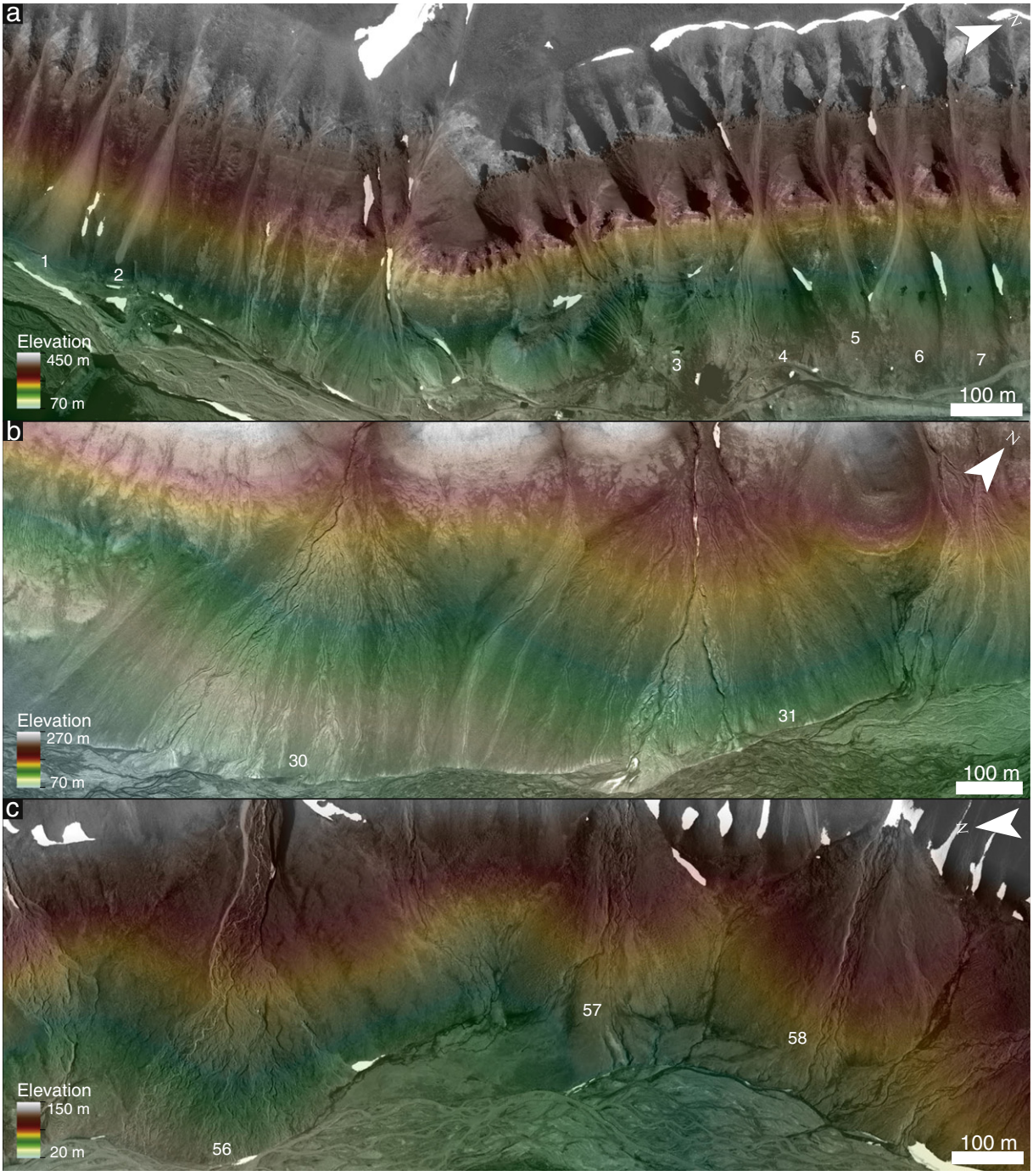

Fig. 4. Fan types in the Adventdalen region. (a) Colluvial fans in Longyeardalen (fans 1–7). (b) Debris-flow-dominated fans in Mälardalen (fans 30–31). (c) Fluvial flow-dominated fans in Bjørndalen (fans 56–58). See Table 1 for corresponding fan numbers and details. Image: HRSC-AX, DLR.

4.1. Morphometry

There is a strong distinction between fan slope versus catchment area, and fan area versus catchment area relations between the rockfall and snow avalanche-, debris-flow- and fluvial-flow-dominated fans on Svalbard (Fig. 5). The colluvial fans have a smaller fan area and catchment area and are steeper than the debris-flow- and fluvial-flow-dominated fans. The slope and area of the debris-flow- and fluvial-flow-dominated fans are in the same range. The main morphometric difference between these two fan types is their catchment: the fluvial-flow-dominated fans have a larger catchment area and a lower slope (Table 1). This implies that the dominant formative process of fans on Spitsbergen is largely determined by catchment morphometry. More rain or meltwater is able to accumulate in larger catchments and less sediment can be entrained because of the lower slope, resulting in a smaller sediment to water ratio and fluvial flows. The morphometry of the fans on Svalbard is within the range observed in various arid to semi-arid regions in Spain and the United States (Harvey, 2011), which suggests that there are no substantial climate-specific differences in large-scale fan morphometry between periglacial and other environments.

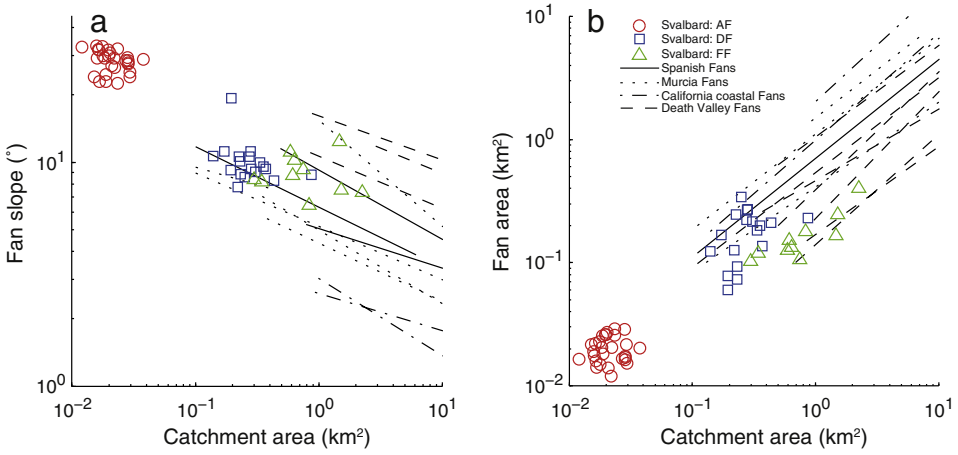

Fig. 5. Comparison between Svalbard fan morphometry and fans in other environments. (a) Fan slope versus catchment area. (b) Fan area versus catchment area. Data from fans in other environments from Harvey (2011). See Table 1 for raw data.

4.2. Snow avalanche-dominated fans

Svalbard hosts many colluvial fans, which have formed by a combination of snow avalanches and rockfall (Fig. 6a, b, d). Although the relative influence of both processes differs between sites, snow avalanches dominate the morphology of the studied colluvial fans. These fans are steep (~29°) and small, and are typically fed by short and steep (~39°) catchments with a sharp plateau edge, where cornice formation and corresponding cornice-fall avalanches are frequent (Table 2). Fan long-profiles are concave, whereas cross-profiles are plano-convex, but with a flattened top because of snow avalanche erosion, especially in the proximal domain of the fans (Fig. 6a–c). The steep mountain walls of the upper catchment and the fan deposits are often dissected by narrow parallel or funnel-shaped snow avalanche chutes. Snow avalanches especially erode large particles that stick out of the surface. Therefore, the proximal fan surface often comprises relatively fine sediments, ranging from clay to small cobbles (Fig. 7e), whereas coarse material, up to 0.5 m in diameter, is deposited on the distal domain of the fans (Figs. 7g and 8). The voids between the pebbles and small cobbles on the proximal domain are filled with fine sediments, as snow avalanche erosion continuously exposes the deeper talus, whereas the coarse material on the distal domain generally has an openwork texture. On the non-flattened sides of the proximal domain of the fan coarse, openwork debris is also abundant, as these parts of the fan are sheltered from snow avalanche erosion. Arcuate alignments of coarse sediment mark the limit of past avalanche activity on some colluvial fans (Fig. 7a). There is a sharp color transition between the freshly exposed proximal domain of the fans and the older, coarse debris along the edges and distal domain of the fans, where sediment has become grayer due to lichen growth and rock varnish. The extensive sediment transport by snow avalanches on the fans is testified by the widespread occurrence of perched cobbles and boulders on all colluvial fans (Fig. 7g). Moreover, debris tails (Fig. 7d) and debris horns (Fig. 7f) were found on the proximal domain of some of the colluvial fans. On distal surfaces where vegetation was removed by snow avalanches, roots were oriented in the flow-direction of the erosive snow avalanches.

On all studied colluvial fans we found many of the above indicators (i.e., flattened cross-profiles, heavily eroded apex region, perched boulders) of extensive snow avalanche activity, suggesting that snow avalanches dominantly affect the morphology of colluvial fans in the Adventdalen region. Siewert et al. (2012) show that the prevailing SE wind direction causes colluvial fans on NW facing slopes to be dominantly aggraded by snow avalanches, whereas the colluvial fans on the SE facing slopes dominantly aggraded by rockfall. This suggests that snow avalanches dominate the surface morphology and texture of all colluvial fans in the region regardless of their dominant aggradational mechanism.

Three out of 31 investigated colluvial fans have a typical tongue-shape (Fig. 7a, b), often referred to as roadbank tongue (Rapp, 1960; Luckman, 1977) or boulder tongue (Jomelli and Francou, 2000). These tongue-shaped deposits have a marked basal concavity of the lower, depositional, part of the fan, and a flat-topped vertical profile, not only in their proximal but also in their distal domain (Fig. 6c). More importantly, the distal domain of the tongue generally has a relatively low-sloping longitudinal profile and the lower edge of the tongue is often marked by a typical step of a few meters in height. As such, these fans have a relatively large difference in apex zone and distal zone angle. Consequently, their average slope can be as low as 15° (Table 2). Whether a cone- or tongue-shaped colluvial fan is formed appears to be controlled by sediment supply. Where sediment supply is high, and a large amount of sediment has accumulated on a fan, snow avalanches continuously rework and bulldoze previously deposited sediment towards the lower fan, eventually forming the marked tongue-shaped deposit. Although deposition or erosion may occur on any part of the tongue per snow avalanche, the overall effect is a net downslope transfer of sediment forming the marked tongue-shaped deposit. On fans where less material has accumulated, no tongue-shaped front develops.

On the majority of the snow avalanche-dominated fans, one or two debris-flow tracks are present originating from the upper parts of the fans, where a mixture of angular debris and fines is exposed. However, after formation the marked relief of the paired levees and depositional lobes is rapidly beveled and leveled by the erosional effect of subsequent snow avalanches. Moreover, where levees still have a marked relief much snow avalanche-transported debris accumulates in between the levees, where it is sheltered from erosion by subsequent snow avalanches. Solifluction and creep are prevalent on the steep snow avalanche-dominated fans in Svalbard (Fig. 9). They transport debris downslope and modify original fan morphology. Solifluction sheets are evident at the base of some of the steep snow avalanche-dominated fans (Fig. 9a). Small solifluction lobes have developed at the surface of some of these fans, but mainly on fans where the primary input of debris from snow avalanches and rockfall is limited (Fig. 9a). On fans where debris supply from snow avalanches and rockfall is larger solifluction occurs probably at similar rates, but is unable to develop lobes. Here, the formation of solifluction lobes is inhibited by the large input of debris by snow avalanches and rockfall together with snow

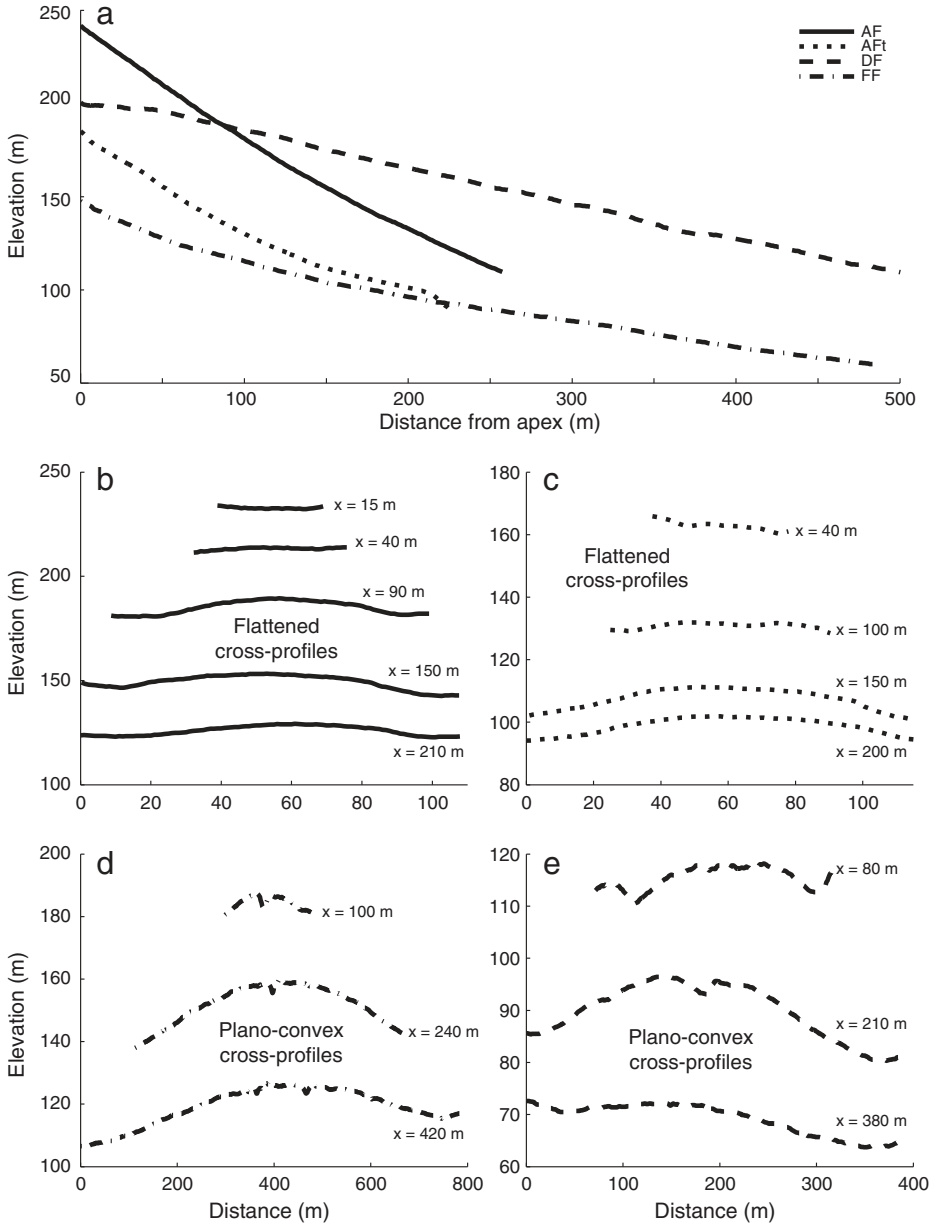

Fig. 6. Topographic profiles (above MSL) of selected examples of the discriminated fan types. (a) Long-profiles of cone-shaped snow avalanche-dominated colluvial fan (AF; fan 7), tongue-shaped snow avalanche-dominated colluvial fan (AFt; fan 53), debris-flow-dominated fan (DF; fan 31) and fluvial-flow-dominated fan (FF; fan 58). (b) Cross-profiles of cone-shaped colluvial fan. (c) Cross-profiles of tongue-shaped colluvial fan. (d) Cross-profiles of debris-flow-dominated fan. (e) Cross-profiles of fluvial-flow-dominated fan. Distance from apex denoted by 'x'. Based on HRSC-AX data.

avalanche erosion. This is illustrated on steep fans in Bjørndalen, where solifluction lobes are absent on the surfaces of snow avalanche fans where deposition and erosive events are frequent, but are present on the less active slopes between these fans (Fig. 9b).

4.3. Debris-flow-dominated fans

The average slope of the investigated debris-flow-dominated fans is 9° and they are typically between 400 and 700 m long and wide

Table 2
Summary of morphometric characteristics per fan type. Total number of investigated fans are given behind fan type abbreviation. Area and slope values are median, minimum and maximum, respectively. See Table 1 for raw data.

Fan type	Fan slope, °	Fan area, m^2	Catchment slope, °	Catchment area, m^2	Long-profile	Cross-profile
AF (28)	29 (23–34)	19,733 (11,366–29,270)	39 (36–43)	20,282 (7489–37,922)	Concave	Plano-convex, with a flattened top
AFt (3)	23 (15–29)	16,098 (16,098–16,805)	32 (32–38)	17,620 (14,151–60,410)	Concave, with marked basal concavity	Plano-convex, with a flattened top
DF (20)	9 (8–19)	175,928 (21,757–341,782)	25 (15–32)	262,764 (139,670–869,820)	Straight to slightly concave	Plano-convex
FF (11)	9 (7–12)	133,935 (77,040–403,853)	11 (7–23)	693,672 (297,860–225,486)	Concave	Plano-convex

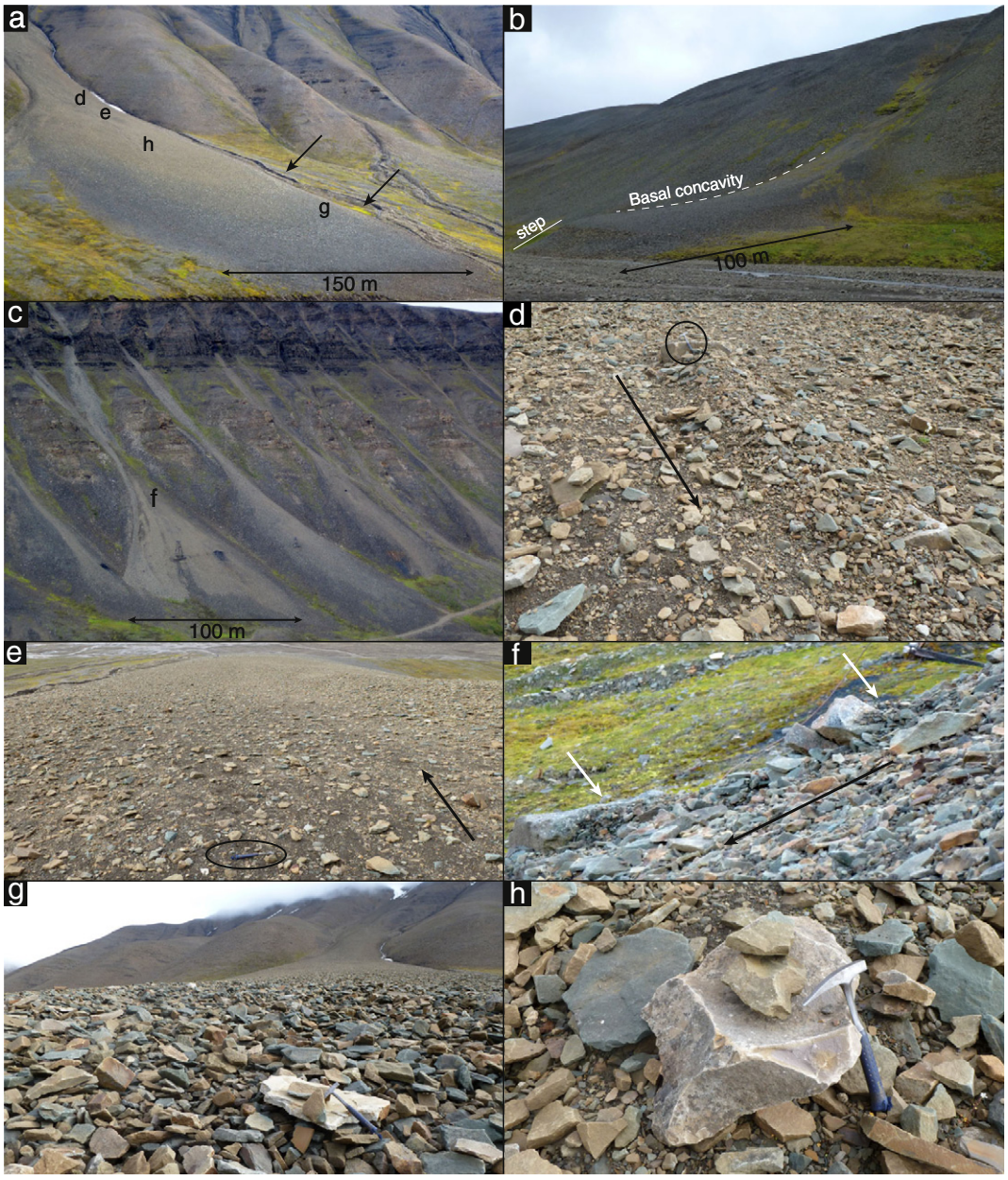

Fig. 7. Snow avalanche-dominated fans. (a) Tongue-shaped snow avalanche fan (32) in Mälardalen. Note the snow avalanche flattened proximal domain, and the more grayish (more lichen) sediment along the sides and lower part of the fan. Arrows denote arcuate alignments of coarse sediment. Letters denote picture locations. (b) Tongue-shaped avalanche fan in Bjørndalen (fan 53). Note that the steepness of the step at the base of the fan is enhanced by basal erosion by the river. (c) Cone-shaped avalanche fans (5–9) in Longyeardalen. (d) Debris tail on the proximal domain of fan 32. Hammer for scale. Black arrow denotes flow direction. (e) Fine-grained texture due to avalanche erosion on the proximal domain of fan 32. Black arrow denotes flow direction. (f) Debris horns on the proximal domain of fan 6 in Longyeardalen. White arrows point at the debris horns, black arrow denotes flow direction. (g) Accumulation of coarse sediment on the distal domain of fan 32. (h) Perched boulder on fan 32.

(Table 2). Longitudinal profiles are straight to slightly concave, and cross-profiles are typically plano-convex (Fig. 6a, d). In a few cases longitudinal profiles are convex in the proximal domain, potentially caused by rockfall or short dry snow avalanche input. Catchment length varies from 800 to 1700 m, and slopes average 25°. The majority of the debris-flow-dominated fans are eroded at their toe by valley-floor braided rivers, and many debris-flow channels reach the distal end of the fans or the valley-bottom braided rivers. Continuous snow and ice melt in the active layer within the catchments during spring and summer feeds small streams that flow through, and erode, the most recent debris-flow tracks on the fan surface. Consequently, these debris-flow tracks become significantly deepened (Fig. 10b, c), and subsequent debris flows are directed and transported within these channels. The small meltwater streams often bifurcate where debris-flow lobes plugged the channel (Fig. 10g). The investigated debris flows are rich in platy debris and clay, as seen in recent debris flows (1–3 days old) observed in Adventdalen, Mälardalen and Hanaskogdalen (Fig. 10d, f). The platy, coarse, debris is provided by the sandstone layers within the catchments, whereas the fines are provided by the shales and siltstones. Due to the platy shape of much of the coarse material, debris-flow lobes often show moderate to good imbrication. Furthermore, many centimeter to decimeter-sized blocks of ice are present within recent deposits, suggesting debris-flow formation by active-layer detachment. The main channel incision near the apex of the fans results in

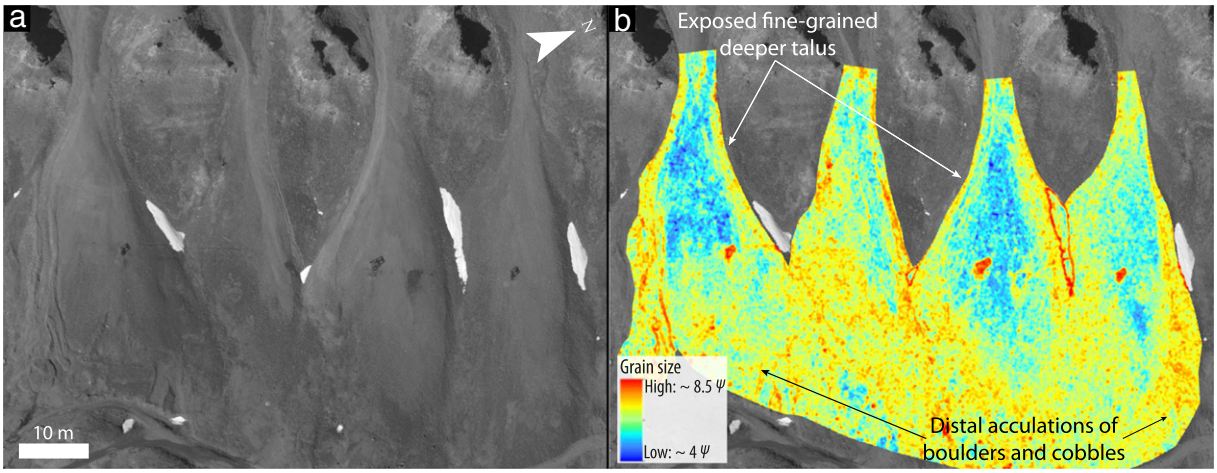

Fig. 8. Surface texture of snow avalanche-dominated colluvial fans in Longyeardalen (fans 4–7). (a) HRSC-AX orthophoto. (b) Grain size maps on top op HRSC-AX orthophoto. Grain-size calibration curve in Fig. 2.

preferential debris-flow activity on a laterally restricted active part of the fan, and in the presence of extensive inactive parts. Levees are generally up to 3 m wide and up to 0.5 m high. However, older levees show much less relief, and ultimately become completely beveled and leveled (Figs. 10e and 11). Relative age estimations from lichenometry (Werner, 1990; Roof and Werner, 2011) indicate that levees become more beveled with increasing age. Beveling and leveling can probably be attributed to the erosive effect of snow avalanches, solifluction and frost weathering, although André (1990a, 1995) mainly attribute it to snow avalanches. No active-layer detachments were found that could be directly linked to debris-flow deposits because we did not investigate the often steep catchments of the fans in the study area. To illustrate the typical morphology of active-layer detachments we show examples found near the mouth of Hanaskogdalen, and on steep slopes near Svea, 60 km south of Longyearbyen in Fig. 12.

The effect of snow avalanches on the fans is twofold, as they erode the fan surface, but can also transport sediment to the fans, as testified by a recent slush-avalanche deposit on the surface of a debris-flow-dominated fan in Adventdalen (Fig. 13), which forms a relatively thin (~10–20 cm), uniform blanket of sediment ranging in size from clay to cobbles and boulders on a large part of the fan. In addition to erosion of debris-flow morphology by snow avalanche erosion on the inactive parts of the fans, they are also heavily influenced by other secondary processes (Fig. 15). Solifluction smooths the surface and causes slow downfan transport of the fan material. Its effect is mainly testified to the formation of solifluction lobes and sheets (vertical step of a few decimeters to a meter) at the distal end of some of the fans (Fig. 15e). Furthermore, ice-wedges and associated polygonal ground (up to ~10 m in diameter) are formed on inactive fan surfaces (Fig. 15a, b), and surface sediments are broken down by frost weathering (Fig. 15f).

4.4. Fluvial-flow-dominated fans

The fluvial-flow-dominated fans have slopes ranging between 7° and 12°, their longitudinal profiles are strongly concave (Fig. 6a, e), while cross-profiles are plano-convex. The fans have a similar size as the debris-flow-dominated fans, whereas their catchments are generally larger (Table. 2). Average catchment slope is 11°. Most fluvial-flow-dominated fans are eroded at their toe by valley-floor braided rivers, and all such fans have a large apex incision (up to 7 m deep) (Fig. 14a, b). In spring and summer there is continuous discharge from the catchments from snow and permafrost melt. The incised morphology of these fans causes a sharp separation between active and inactive sectors on the fan. The active part shows a typical braided planform (Fig. 14b, c). The low flow is often critical or supercritical with many static hydraulic jumps over immobile sediment and infrequent flow bifurcations on an otherwise dry fan surface. Grain size on the fans varies from clay, silt and sand to cobbles of 20–30 cm in diameter at maximum, and the largest fractions are clearly imbricated (Fig. 14d). Sorting is quite patchy at scales smaller than typical bar wavelengths. Bar heads

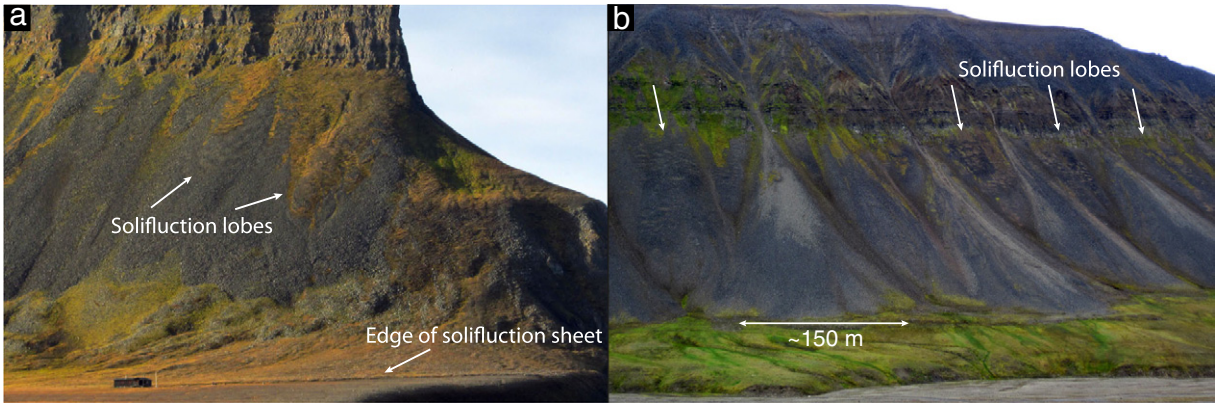

Fig. 9. Solifluction lobes on fans. (a) Solifluction lobes on relatively inactive snow avalanche- and rockfall-dominated fans at the western side of Bjørndalen. A sharp-edged solifluction sheet is present at the foot of the fans. (b) Solifluction lobes on steep slopes between snow-avalanche dominated fans in Bjørndalen (fans 50–52).

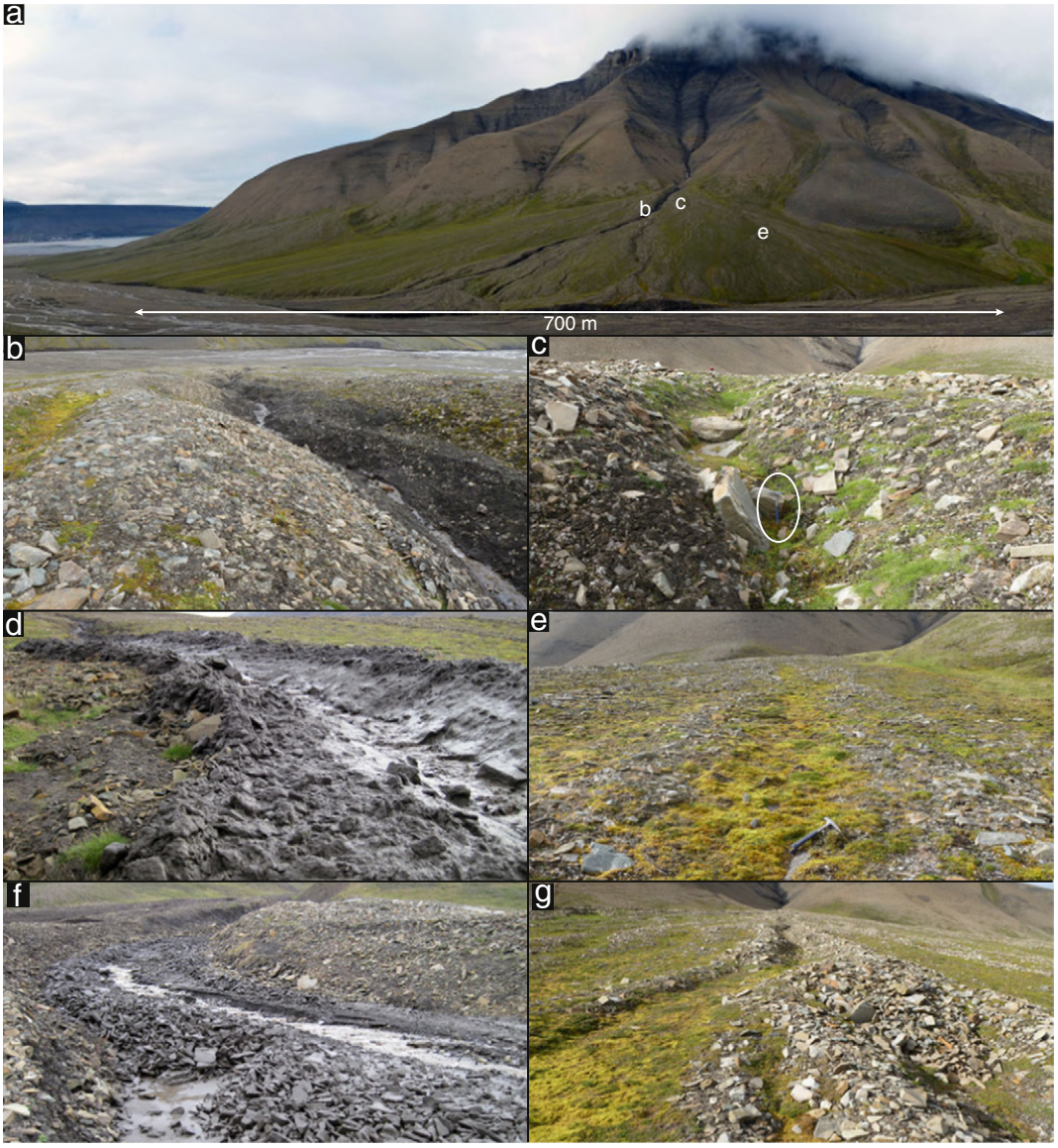

Fig. 10. Debris-flow-dominated fans. (a) Debris-flow-dominated fan (31) in Mälardalen. (b) Debris-flow channel, incised by meltwater stream. (c) Formerly incised debris-flow channel. Step-pool morphology implies reworking by runoff. Hammer for scale. (d) Very recent (1–3 days) debris flow on fan 30. (e) Heavily beveled debris flow on fan 31. (f) Very recent (1–3 days) debris flow on fan 34. (g) Bifurcated meltwater stream in debris-flow channel on fan 31. Meltwater streams often bifurcate and leave debris-flow channels where flow is ponding behind a debris-flow lobe.

are often heavily armored by coarse, imbricated sediment, while backwaters preserved finer sediments. The inactive part of the fans is smoother, most likely because of avalanche erosion, is often vegetated and hummocks (up to ~5 m in diameter) and ice-wedge polygons are present on long-inactive areas (Figs. 14e and 15c, d). On some fluvial-flow-dominated fans there is also a significant geomorphic contribution of slush avalanches, as evidenced by recent snow avalanche deposits on some of these fans (Fig. 13c).

5. Discussion

5.1. Unique morphology and morphometry of fans in periglacial environments

Our results show that snowfall and associated recurrent snow avalanches, continuous permafrost and frequent freeze–thaw cycles result in a unique morphology of fans on Svalbard. This is in contrast with previous studies that suggested that processes leading to alluvial-fan deposits differ little between different environments (e.g., Brierley et al., 1993; Harris and Gustafson, 1993; Ibbeken et al., 1998; Webb and Fielding, 1999; Krzyszkowski and Zieliński, 2002; Harvey et al., 2005; Lafortune et al., 2006). The surface morphology and texture of the studied colluvial fans are strongly affected by snow avalanches, in contrast to the rockfall-dominated morphology and texture of colluvial fans in other regions. Snow avalanches can also contribute sediment to and modify the primary morphology of debris-flow- and fluvial-flow-dominated alluvial fans. The inactive surfaces of these alluvial fans are rapidly beveled and leveled, mainly by snow avalanches, but also by solifluction and frost weathering. Periglacial reworking, such as the formation of ice-wedge polygons and hummocks, further modifies these inactive surfaces. Below we elaborate on the uniqueness of the morphology and texture of fans in the periglacial environment of Svalbard.

In general, the morphology of individual fluvial or debris-flow deposits on fans on Svalbard is similar to the morphology of these deposits in other environments, as found by Catto (1993), Harris and Gustafson

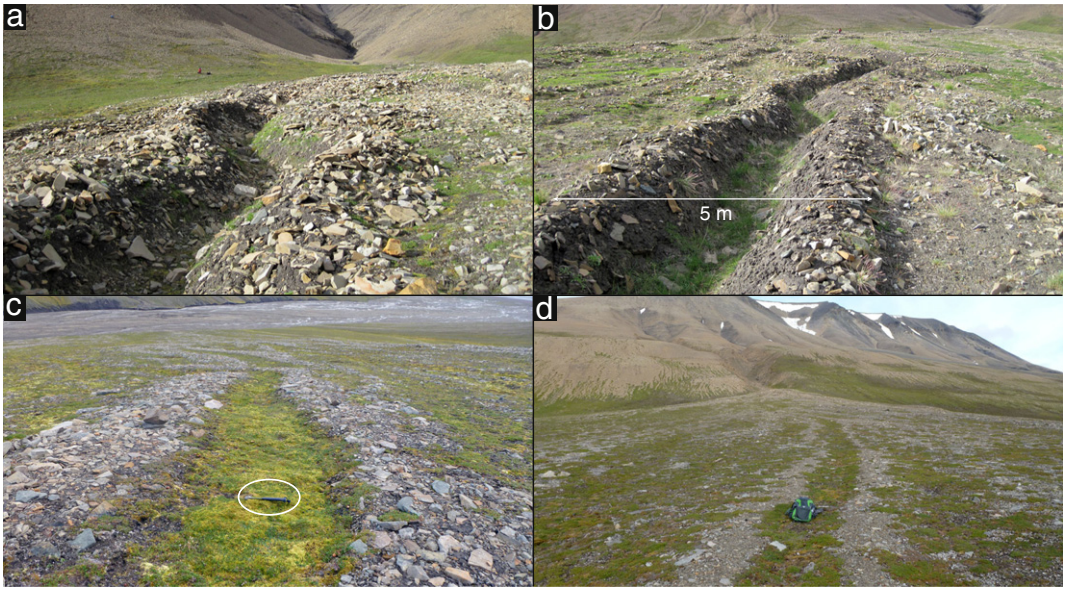

Fig. 11. Debris-flow channels of different ages and degrees of beveling. (a, b) Relatively young debris-flow channels, with pronounced levees and deepened channels by meltwater erosion. Picture a is taken on fan 30, picture b on fan 31 in Mälardalen. (c, d) Relatively old, heavily beveled debris-flow channels, on which relief is decreased to <10 cm. Picture c from fan 30 in Mälardalen, and picture d from fan 40 in Adventdalen (Table 1).

(1993) and Webb and Fielding (1999). However, debris-flow size is often restricted by active-layer depth (André, 1990a). Additionally, during summer months fluvial and especially debris flows are relatively more abundant on Svalbard and many other periglacial regions compared to other climatic regions. Fan surfaces are completely frozen and covered by snow during winter, and therefore fan activity is limited to the spring and summer months (Webb and Fielding, 1999). Consequently, geomorphic activity is more intense during the melting season as snowmelt and rainfall concordantly provide discharge to the fans, and fluvial and debris flows can be triggered by a combination of thawing of snow and ground ice and intense or longlasting rainfall (Decaulne and Sæmundsson, 2007). Moreover, rainfall and/or snowmelt thresholds for debris-flow initiation are low and debris flows are easily triggered because of the permafrost table acting as an aquiclude (e.g., Caine, 1980; Larsson, 1982; Sattler et al., 2011), especially in fine-grained Arctic soils (e.g., Harris and Lewkowicz, 2000; Lewkowicz and Harris, 2005).

Snow avalanches can be an important depositional mechanism on fans in periglacial (e.g., Blikra and Nemec, 1998; Decaulne and Sæmundsson, 2006; Siewert et al., 2012; Eckerstorfer et al., 2013) and Alpine environments (e.g., Jomelli and Francou, 2000; Jomelli and Bertran, 2001). On Svalbard, snow avalanches were found to be an important geomorphic agent on fans, resulting in morphology that significantly differs from the morphology of fans in environments where snow avalanches are less abundant or absent. The snow avalanche-dominated fans are formed below typical snow avalanches chutes and have a flattened cross-profile and sometimes a distinct basal concavity. There is a marked downstream coarsening grain size (Fig. 8), but in contrast to rockfall-dominated colluvial fans, which generally have a more openwork texture (e.g., Friend et al., 2000; Ventra et al., 2013), the voids on the proximal domain are filled with fine sediments, as snow avalanche erosion continuously exposes the deeper talus, and only the coarser-grained distal domain has an openwork texture. Small-scale morphological traits, such as perched cobbles and boulders, debris horns, debris tails and arcuate alignments of coarse debris, exclusively formed by snow avalanches are present on these fans. In the Adventdalen region on Svalbard, we only found snow avalanche-dominated colluvial fan surfaces. Yet, such a strong snow avalanche influence on colluvial fans is probably not representative for all periglacial environments, as the plateau mountains and strong and continuous winds in the Adventdalen region favor the formation of cornices, and cornice-fall avalanches (Eckerstorfer et al., 2013). For example, snow avalanches frequently occur in many of the moderately humid to humid high-latitude northern hemisphere mountains (e.g., Rapp,

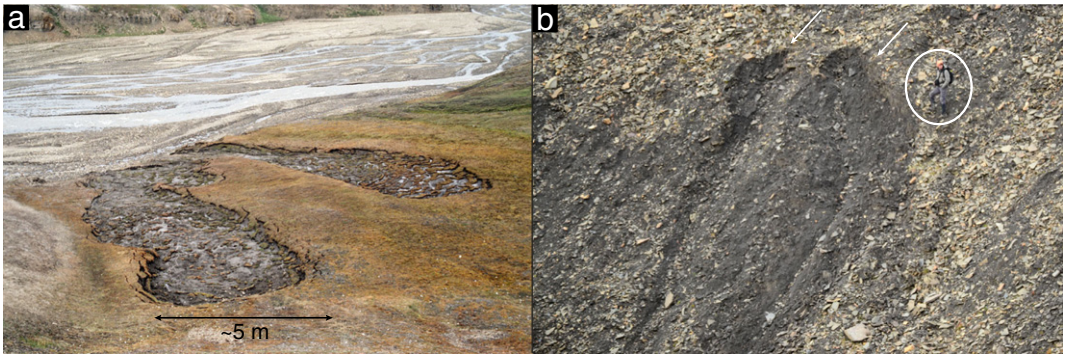

Fig. 12. Examples of active layer detachment. (a) Active-layer detachment or thaw slump near the mouth of Hanaskogdalen. (b) Active-layer detachment on a steep slope near the mining town of Svea.

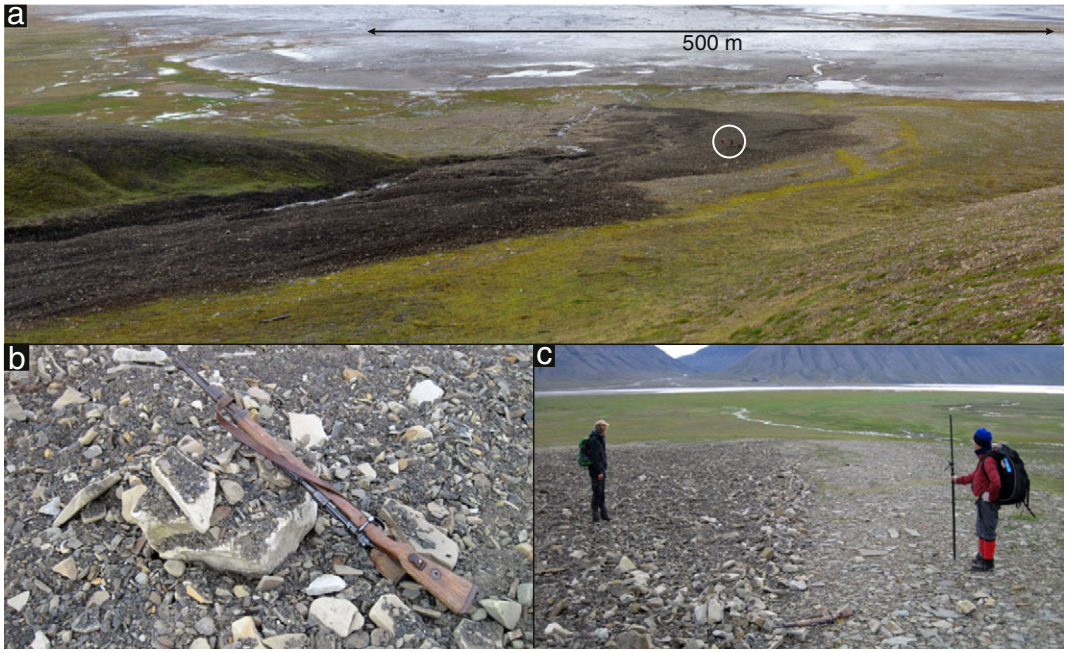

Fig. 13. Recent slush-avalanche deposits. (a) Recent slush-avalanche deposit (<0.5 years) on a debris-flow-dominated fan in Adventdalen (fan 34; Table. 1). (b) Detail of slush-avalanche deposit, showing the wide range of sediment that was transported within the avalanche, and a prominent perched boulder. (c) Slush avalanche on a fan in Adventdalen, indicating the limited thickness of such deposits (~10–20 cm) (not in Table 1).

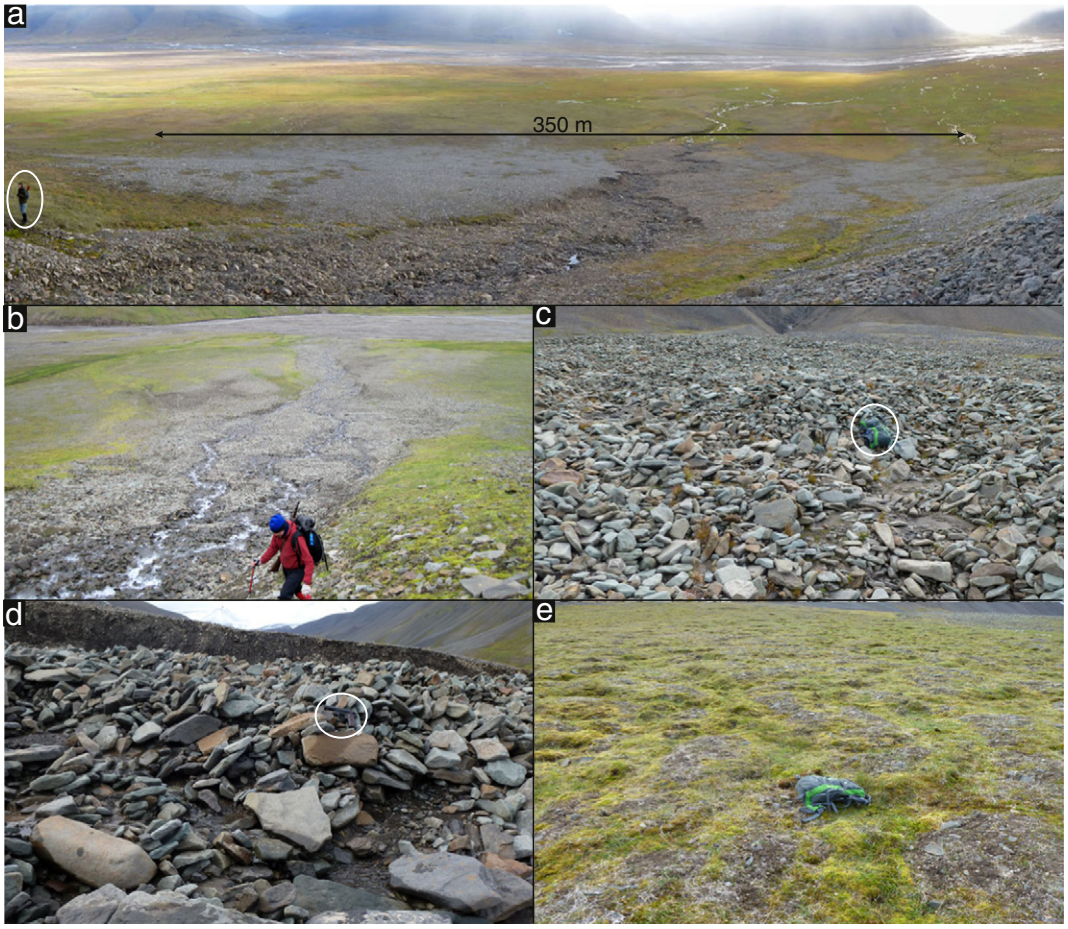

Fig. 14. Fluvial-flow-dominated fans. (a) Fluvial-flow-dominated fan in Adventdalen (fan 38). (b) Fluvial-flow-dominated fan in Bjørndalen (fan 58). These fans are generally incised, separating the active part of the fan from the inactive part. The active part generally has typical braided planform due to the continuous discharge of meltwater in spring and summer. (c) Upfan view on the active part of fan 56. (d) Active part of fan 56, showing clast imbrication. Flare gun for scale. (e) Inactive fan surface of fan 57, the initial morphology is heavily modified and hummocks have formed (Fig. 15c, d).

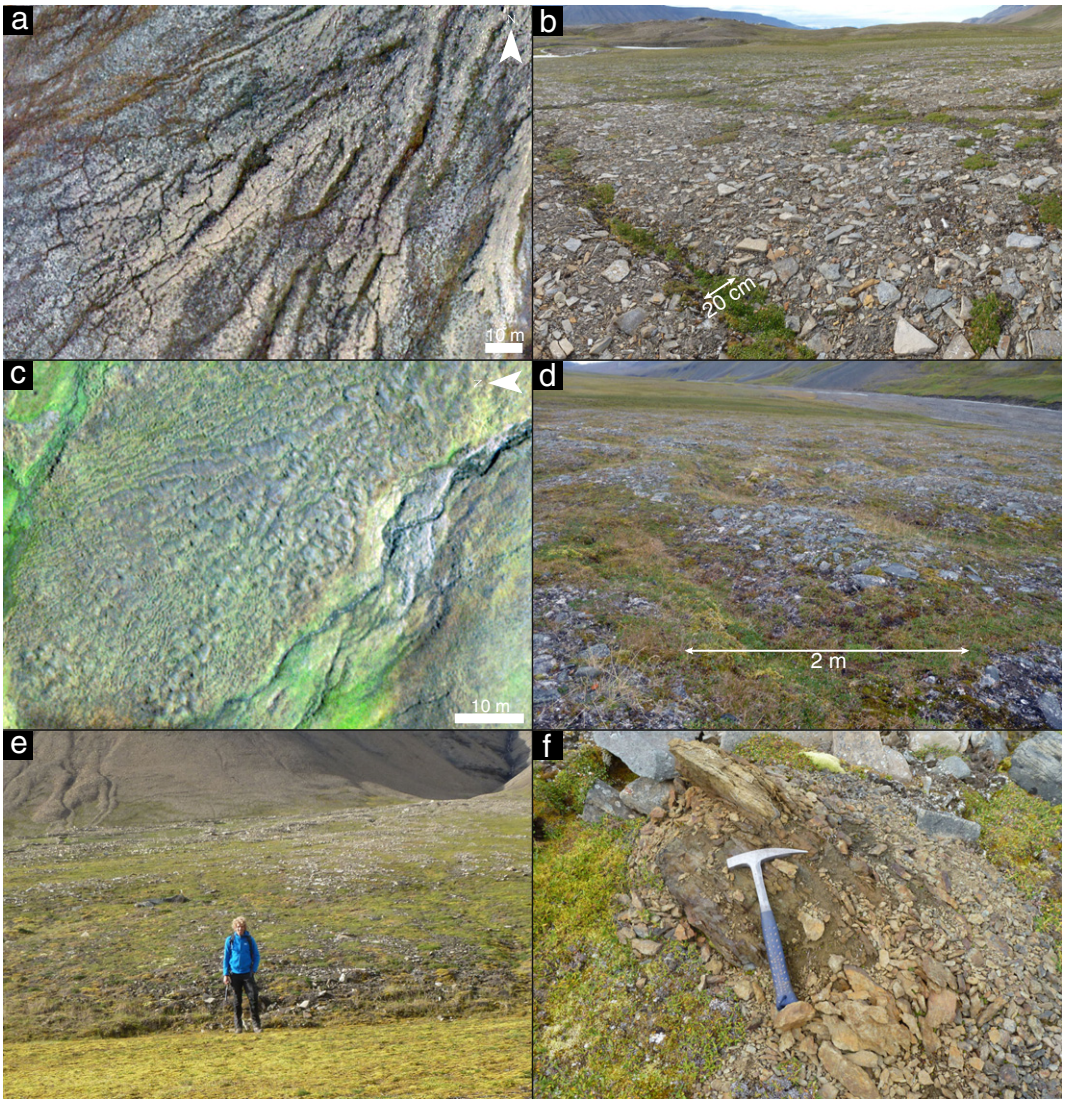

Fig. 15. Morphology of inactive fan surfaces. (a) Polygonal ground on inactive fan surface of debris-flow-dominated fan in Adventdalen (fan 37). (b) Ground picture of polygonal ground shown in picture a. (c) Hummocks on inactive fan surface of a fluvial-flow-dominated fan in Bjørndalen (fan 57). (d) Ground picture of hummocks in picture c. (e) Stepped profile formed by solifluction at the foot of the inactive surface of fan 30 in Mälardalen. (f) Heavily fractured cobble by frost-weathering on fan 31 in Mälardalen.

1985; Luckman, 1992), but scarcely occur on drier regions such as Antarctica. The primary effect of snow avalanches on fluvial and debris-flow-dominated fans is much smaller than on colluvial fans, as snow avalanches are less frequent because of lower sloping catchments. However, snow avalanches were also found to contribute sediment to these fans, mainly in form of slush avalanches, and can consequently have a profound effect on the surface morphology.

The secondary processes causing post-depositional modification and their resulting morphology in the periglacial environment of Svalbard differ from those in other environments, and are mainly associated with snow avalanches, presence of permafrost and freeze–thaw cycles. Frost weathering breaks down surficial clasts, but remnants of broken-down debris are far less abundant than commonly observed on fans in arid to semi-arid environments (e.g., De Haas et al., 2014). Because of snow avalanche erosion, solifluction and weathering, primary morphological features, especially debris-flow lobes and levees, are generally short-lived landforms on inactive fan sectors on Svalbard. André (1990a, 1995) found that recurrent snow avalanches rapidly erode, bevel and level the debris-flow levees and lobes on some fans, and consequently their life span can be as low as 30–40 years. In contrast, on slopes without snow avalanche chutes above, deposits can be preserved much longer, for several centuries and locally more than a millennium (André, 1990a). Similarly, debris-flow levees were almost completely leveled in a 20 year period due to snow avalanche activity in the Cairngorm Mountains in Scotland (Luckman, 1992). The vulnerability of fans to snow avalanche erosion is strongly influenced by the dominant wind direction, as leeward slopes are much more prone to snow avalanches (André, 1995; Eckerstorfer and Christiansen, 2011b; Siewert et al., 2012; Eckerstorfer et al., 2013).

In addition to the extensive fan modification by snow avalanches, solifluction was found to affect the fan surfaces, and on some fans extensive areas with hummocks and/or ice-wedge polygons developed (Fig. 15). Similarly, hummocks also form on the inactive domain of fans in the semi-arid periglacial climate of the Aklavik Range, Canada, with continuous permafrost (Legget et al., 1966; Catto, 1993). However, Webb and Fielding (1999) found that fans in Antarctica experienced only small amounts of post-depositional modification, restricted to wind ablation and limited runoff. In contrast, in arid to semi-arid environments inactive fan surfaces are commonly reworked into a very different morphology. Here, inactive surfaces are often heavily modified by a combination of weathering (mainly salt weathering), runoff and wind erosion (e.g., Wells et al., 1987; Blair and McPherson, 2009; De Haas

et al., 2014). These processes decrease the relief on the inactive fan surfaces and break down surface sediments, ultimately resulting in smooth and homogeneous desert pavement (e.g., Al-Farraj and Harvey, 2000; Frankel and Dolan, 2007). Moreover, as post-depositional smoothing of primary relief can occur within a few decades (André, 1990a, 1990b; Luckman, 1992), post-depositional modification can be a much faster process in periglacial environments than in arid to semi-arid environments, where this generally takes thousands to hundreds of thousands years (Matmon et al., 2006; Frankel and Dolan, 2007).

On Svalbard, and in many other recently deglaciated periglacial regions, fluvial-flow-dominated fans often have a large fanhead incision (Ryder, 1971; Owen and Sharma, 1998; Lønne and Nemec, 2004), which is generally ascribed to a decrease in sediment supply after an initial paraglacial increase since deglaciation of the valleys. However, although this is a valid explanation for the large fanhead incision in these environments, fanhead incisions are common in many other environments (e.g., Nicholas et al., 2009), as besides changes in sediment supply, tectonic uplift (Alexander and Leeder, 1987), and autogenic behavior (Nicholas et al., 2009; Van Dijk et al., 2012) can also cause fanhead incision. Moreover, long-term climate changes could cause similar effects, especially when affecting precipitation amounts.

The large-scale morphometry of fans in the periglacial environment of Svalbard differs insignificantly from the morphometry of fans in various arid to semi-arid regions (Harvey, 2011) (Fig. 5). On a smaller scale, the cross-sectional architecture of the investigated colluvial fans on Svalbard differs from the cross-sectional architecture of colluvial fans in many other environments (e.g., Blair and McPherson, 2009), by its flattened cross-profile caused by frequent snow-avalanche erosion (Fig. 6b–c). Moreover, snow avalanche-dominated fans have a larger difference in apex-zone angle compared to distal-zone angle, then rockfall-dominated colluvial fans (Jomelli and Francou, 2000) (Fig. 6a).

5.2. Future development of fans in periglacial environments

Global warming effects will be profound in the Arctic (e.g., Christiansen et al., 2010; Førland et al., 2012). Svalbard is especially sensitive to atmospheric and oceanic changes, due to its location at the northern margins of the warm North-Atlantic ocean current (e.g., Aagaard and Carmack, 1989). In the last decades, mean annual temperatures increased by ~1 °C per decade, while winter warming was even more dramatic with an increase of ~2–3 °C per decade (Førland et al., 2012). Mean annual precipitation has increased with 2–4% per decade (Førland et al., 2012). As a result, the temperature of the permafrost surface increased by approximately 0.07 °C yr^{-1} in the last decades, with indications of recent accelerated warming (Isaksen et al., 2007). Global Circulation Models predict a 4–6 °C warming and a 5% precipitation increase in Svalbard by 2100 in the SRES A1b emission scenario (Benestad, 2005). This will result in warming of ~4 °C in the near surface layers (<10 m depth) and a dramatic increase in active-layer thickness (Etzelmüller et al., 2011).

Geomorphic activity on steep snow avalanche-dominated colluvial fans is mainly influenced by the dominant winter wind direction (Siewert et al., 2012; Christiansen et al., 2013; Eckerstorfer et al., 2013), as this determines the favorable slopes for snow-cornice accretion, and fills the mountain ravines and gullies with thick snowpacks that may later obstruct runoff, causing slush avalanches (Blikra and Nemec, 1998). Hence, an increase in average temperature will not directly affect the colluvial fans on Svalbard, rather potential climate-induced changes in precipitation amount and dominant winter wind direction will adjust snow avalanche sedimentation. Changes in winter wind direction will probably lead to changes in the location of areas with extensive snow avalanche sedimentation and thus snow avalanche fans and rock glaciers (Eckerstorfer et al., 2013). As precipitation rates in the Arctic have roughly increased by 14% in the last century and greatest increases were observed in autumn and winter (Førland et al., 2012), cornice formation and corresponding snow avalanche erosion and sedimentation will probably increase, leading to higher geomorphic activity on the colluvial fans. Especially an increase in the number of days with high amounts of precipitation in winter may lead to a higher snow-avalanche frequency (Laute and Beylich, 2014), and wet snow avalanches most likely become more frequent when the rain-on-snow events during the winter season increase (Kronholm et al., 2006; Laute and Beylich, 2014). In general, the increase in active-layer depth on Svalbard during recent years, and especially during the last decades is similar to observations in other periglacial regions (e.g., Christiansen et al., 2010; Romanovsky et al., 2010; Smith et al., 2010). Rising air temperatures in the Arctic regions and anticipated deeper active layers, will cause thaw to advance into ice-rich frozen ground that has not thawed for many decades, centuries or even millennia (Isaksen et al., 2007; Harris et al., 2009), thereby increasing the amount of sediment available for transport due to loss of soil stabilizing ice (e.g., Zimmermann and Haeberli, 1993; Bardou et al., 2011; Schoeneich et al., 2011) and the probability of soil failure and debris-flow initiation by a reduction of soil shear strength (Nater et al., 2008; Rist, 2008; Harris et al., 2011; Sattler et al., 2011). In consequence, there will likely be a marked increase in both the rates of solifluction and the volume of annual sediment transport due to an increase in debris-flow frequency on Svalbard (Matsuoka, 2001; Åkerman, 2005; Harris et al., 2011). The anticipated increased precipitation frequency and magnitude will further increase debris-flow frequency (Rebetez et al., 1997; Huscroft et al., 2003). Additionally, an increase in active-layer thickness will increase debris-flow volume (Rist, 2008; Clague et al., 2012), especially as André (1990a) indicates that the size of debris flows on Svalbard is currently limited by the active-layer depth. Thus, climatic change on Svalbard is likely to increase the frequency and magnitude of geomorphic events on fans. Moreover, ongoing deglaciation will expose an increasing amount of slopes yielding large volumes of sediment ready for transport to hillslopes and alluvial fans (Mercier et al., 2009). The increase of coarse sediment supply may have adverse effects on the rivers in the valleys and the increase of fine sediment supply to the fjords and coastal waters may adversely affect the marine ecosystem.

Although the above analysis focuses on the geomorphic effects of global warming on Svalbard, we anticipate a similar response in other Arctic, Antarctic and periglacial environments. However, the exact geomorphic response is site-specific and depends on local climatic response to global warming (e.g., Pavlova et al., 2014).

6. Conclusions

We studied the effects of periglacial conditions on the morphology of snow avalanche-dominated colluvial fans, and debris-flow- and fluvial-flow-dominated fans on Svalbard on the basis of new data and literature review. Both snow avalanches and rockfall contribute significant amounts of debris to colluvial fans, but snow avalanches were found to dominate surface morphology and morphometry of the investigated colluvial fans. These fans have flattened cross-profiles and fine-grained proximal domains due to avalanche erosion, whereas the distal domains primarily consist of cobbles and boulders with an openwork texture. On a smaller scale the extensive snow avalanche activity is testified by the presence of perched cobbles and boulders and debris horns and tails. In a few cases, where loose sediment and snow avalanches are abundant, tongue-shaped colluvial fans are formed. Snow avalanche-dominated colluvial fans are absent in most other environments on Earth, where they generally form by rockfall.

The large-scale morphometry (e.g., catchment and fan area and slope) of debris-flow- and fluvial-flow-dominated alluvial fans on Svalbard is similar to those in most other environments on Earth. The primary deposits of debris flows and fluvial flows are largely similar to those in other environments, but the interaction of these processes with periglacial processes on the fans leads to a unique morphology. Snow avalanches contribute significant amounts of sediment to debris-flow- and fluvial-flow-dominated fans and modify both

morphology and sediment size-sorting patterns. On these fans, snow avalanches often have enough erosive power to bevel and level the primary relief and reduce the sediment size-sorting formed by the debris flows and fluvial flows. Frost weathering and solifluction probably contribute to smoothing of the fan morphology. On the longer term, ice wedge polygonal ground, hummocks and solifluction sheets and lobes form on inactive fan surfaces, removing the primary relief.

The intense global warming in Arctic regions will most likely enhance geomorphic activity on alluvial fans in these regions, as increased summer precipitation (rain) and permafrost degradation will probably enhance debris-flow frequency and magnitude. On the other hand, activity on colluvial fans is most likely mainly influenced by shifts in dominant winter wind direction and resulting snow avalanche activity.

Supplementary data to this article can be found online at http://dx.doi.org/10.1016/j.earscirev.2015.04.004.

Acknowledgments

This work is part of the PhD research of TdH, supported by the Netherlands Organisation for Scientific Research (NWO) and the Netherlands Space Office (NSO) (grant ALW_GO_PL17_2012 to MGK). We gratefully acknowledge the Norwegian Polar Institute (NPI) for logistical support during fieldwork. Special thanks go to Jørn Dybdahl of NPI for help with planning and logistics, including all boat transports to and from the field sites and to other aids to our survival. We further acknowledge DLR for the use of the HRSC-AX data and Kolibri Geo Services for the high-resolution aerial images of fans in Adventdalen. Constructive comments by Christopher R. Fielding and one anonymous reviewer are gratefully acknowledged. The authors contributed in the following proportions to conception and study design, data collection, analysis and conclusions, and manuscript preparation: TdH (40, 30, 60, 60)%, MGK (30, 30, 20, 20)%, PEC (20, 30, 0, 0)%, LR (0, 0, 10, 10)%, EH (10, 10, 10, 10)%.

References

Aagaard, K., Carmack, E., 1989. The role of sea ice and other fresh water in the Arctic circulation. J. Geophys. Res. Oceans (1978–2012) 94 (C10), 14485–14498.
Agisoft, 2011. Image-based 3D modelling. Available at: www.agisoft.ru.
Åkerman, H.J., 1984. Notes on talus morphology and processes in Spitsbergen. Geogr. Ann. Ser. A Phys. Geogr. 66 (4), 267–284.
Åkerman, H.J., 2005. Relations between slow slope processes and active-layer thickness 1972–2002, Kapp Linné, Svalbard. Nor. Geogr. Tidsskr. 59 (2), 116–128.
Alexander, J., Leeder, M.R., 1987. Recent developments in fluvial sedimentology. Society of Economic Paleontologists and Mineralogists Special Publication 39, Ch. Active tectonic control on alluvial, architecture. pp. 234–252.
Al-Farraj, A., Harvey, A.M., 2000. Desert pavement characteristics on wadi terrace and alluvial fan surfaces: Wadi Al-Bih, U.A.E. and Oman. Geomorphology 35 (34), 279–297.
André, M.-F., 1986. Dating slope deposits and estimating rates of rock wall retreat in northwest Spitsbergen by lichenometry. Geogr. Ann. Ser. A Phys. Geogr. 68 (1/2), 65–75.
André, M.-F., 1990a. Frequency of debris flows and slush avalanches in Spitsbergen: a tentative evaluation from lichenometry. Pol. Polar Res. 11, 345–363.
André, M.-F., 1990b. Geomorphic impact of spring avalanches in northwest Spitsbergen (79 N). Permafr. Periglac. Process. 1 (2), 97–110.
André, M.-F., 1995. Holocene climate fluctuations and geomorphic impact of extreme events in Svalbard. Geogr. Ann. 77 (4), 241–250.
André, M.-F., 1997. Holocene rockwall retreat in Svalbard: a triple-rate evolution. Earth Surf. Process. Landf. 22 (5), 423–440.
André, M.-F., 2003. Do periglacial landscapes evolve under periglacial conditions? Geomorphology 52 (1), 149–164.
Ballantyne, C.K., 2002. Paraglacial geomorphology. Quat. Sci. Rev. 21 (18), 1935–2017.
Bardou, E., Favre-Bulle, G., Ornstein, P., Rouiller, J.D., 2011. Influence of the connectivity with permafrost of the debris-flow triggering in high-Alpine environment. Ital. J. Eng. Geol. Environ. 10, 13–21.
Benestad, R., 2005. Climate change scenarios for northern Europe from multi-model IPCC AR4 climate simulations. Geophys. Res. Lett. 32 (17), L17704.
Bibus, E., 1975. Geomorphologische Untersuchungen zur Hang-und Talentwicklung im zentralen West-Spitzbergen. Polarforschung 45 (2), 102–119.
Blair, T.C., 1999. Sedimentology of the debris-flow-dominated Warm Spring Canyon alluvial fan, Death Valley, California. Sedimentology 46 (5), 941–965.
Blair, T.C., McPherson, J.G., 1994. Alluvial fans and their natural distinction from rivers based on morphology, hydraulic processes, sedimentary processes, and facies assemblages. J. Sediment. Res. 64A, 450–489.
Blair, T.C., McPherson, J.G., 2009. Processes and forms of alluvial fans. In: Parsons, A., Abrahams, A. (Eds.), Geomorphology of Desert Environments. Springer, Netherlands, pp. 413–467.
Blikra, L.H., Nemec, W., 1998. Postglacial colluvium in western Norway: depositional processes, facies and palaeoclimatic record. Sedimentology 45 (5), 909–960.
Bogen, J., Bønsnes, T.E., 2003. Erosion and sediment transport in High Arctic rivers, Svalbard. Polar Res. 22 (2), 175–189.
Brazier, V., Whittington, G., Ballantyne, C.K., 1988. Holocene debris cone evolution in Glen Etive, Western Grampian Highlands, Scotland. Earth Surf. Process. Landf. 13 (6), 525–531.
Brierley, G.J., Liu, K., Crook, K.A., 1993. Sedimentology of coarse-grained alluvial fans in the Markham Valley, Papua New Guinea. Sediment. Geol. 86 (3), 297–324.
Brown, J., Ferrians, O.J., Heginbottom, J., Melnikov, E., 1997. Circum-Arctic map of permafrost and ground-ice conditions. US Geological Survey Map CP-45, Circum-Pacific Map Series, scale 1:10,000,000.
Bryant, I.D., 1982. Loess deposits in lower Adventdalen, Spitsbergen. Polar Res. 1982 (2), 93–103.
Caine, N., 1980. The rainfall intensity-duration control of shallow landslides and debris flows. Geogr. Ann. A 62 (1–2), 23–27.
Carbonneau, P.E., 2005. The threshold effect of image resolution on image-based automated grain size mapping in fluvial environments. Earth Surf. Process. Landf. 30 (13), 1687–1693.
Carbonneau, P.E., Lane, S.N., Bergeron, N.E., 2004. Catchment-scale mapping of surface grain size in gravel bed rivers using airborne digital imagery. Water Resour. Res. 40 (7), W07202.
Catto, N.R., 1993. Morphology and development of an alluvial fan in a permafrost region, Aklavik Range, Canada. Geogr. Ann. Ser. A Phys. Geogr. 75 (3), 83–93.
Cavalli, M., Marchi, L., et al., 2008. Characterisation of the surface morphology of an Alpine alluvial fan using airborne LiDAR. Nat. Hazards Earth Syst. Sci. 8 (2), 323–333.
Chiverrell, R., Harvey, A., Foster, G., 2007. Hillslope gullying in the Solway Firth-Morecambe Bay region, Great Britain: responses to human impact and/or climatic deterioration? Geomorphology 84 (3), 317–343.
Christiansen, H.H., Etzelmüller, B., Isaksen, K., Juliussen, H., Farbrot, H., Humlum, O., Johansson, M., Ingeman-Nielsen, T., Kristensen, L., Hjort, J., et al., 2010. The thermal state of permafrost in the Nordic area during the International Polar Year 2007–2009. Permafr. Periglac. Process. 21 (2), 156–181.
Christiansen, H.H., Humlum, O., Eckerstorfer, M., 2013. Central Svalbard 2000–2011 meteorological dynamics and periglacial landscape response. Arct. Antarct. Alp. Res. 45 (1), 6–18.
Clague, J.J., Huggel, C., Korup, O., McGuire, B., 2012. Climate change and hazardous processes in high mountains. Rev. Asoc. Geol. Argent. 69 (3), 328–338.
Dallmann, W., Kjærnet, T., Nøttvedt, A., 2001. Geomorphological and quaternary map of Svalbard. Norsk Polarinstitutt Temakart 31/32, scale 1:100,000.
Dallmann, W., Ohta, Y., Elvevold, S., 2002. Bedrock map of Svalbard and Jan Mayen. Norsk Polarinstitutt Temakart 33, scale 1:750,000.
Davies, T.R., Smart, C.C., Turnbull, J.M., 2003. Water and sediment outbursts from advanced Franz Josef glacier, New Zealand. Earth Surf. Process. Landf. 28 (10), 1081–1096.
De Haas, T., Hauber, E., Kleinhans, M.G., 2013. Local late Amazonian boulder breakdown and denudation rate on Mars. Geophys. Res. Lett. 40, 35273531.
De Haas, T., Ventra, D., Carbonneau, P.E., Kleinhans, M.G., 2014. Debris-flow dominance of alluvial fans masked by runoff reworking and weathering. Geomorphology 217, 165–181.
Decaulne, A., Sæmundsson, T., 2003. Debris-flow characteristics in the Gleidarhjalli area, northwestern Iceland. Debris-flow Hazards Mitigation: Mechanics, Prediction, and Assessment 2 pp. 1107–1118.
Decaulne, A., Sæmundsson, T., 2006. Geomorphic evidence for present-day snow-avalanche and debris-flow impact in the Icelandic Westfjords. Geomorphology 80 (1), 80–93.
Decaulne, A., Sæmundsson, T., 2007. Spatial and temporal diversity for debris-flow meteorological control in subarctic oceanic periglacial environments in Iceland. Earth Surf. Process. Landf. 32 (13), 1971–1983.
Derbyshire, E., Owen, L.A., 1990. Quaternary alluvial fans in the Karakoram Mountains. Alluvial Fans: A Field Approach. Wiley, Chichester, pp. 27–53.
Dorn, R.I., 1994. The role of climatic change in alluvial fan development. Geomorphology of Desert Environments. Springer, pp. 593–615.
Eckerstorfer, M., Christiansen, H.H., 2011a. The "high Arctic maritime snow climate" in central Svalbard. Arct. Antarct. Alp. Res. 43 (1), 11–21.
Eckerstorfer, M., Christiansen, H.H., 2011b. Topographical and meteorological control on snow avalanching in the Longyearbyen area, central Svalbard 2006–2009. Geomorphology 134 (3), 186–196.
Eckerstorfer, M., Christiansen, H.H., 2012. Meteorology, topography and snowpack donditions causing two extreme mid-winter slush and wet slab avalanche periods in high Arctic maritime Svalbard. Permafr. Periglac. Process. 23 (1), 15–25.
Eckerstorfer, M., Christiansen, H.H., Vogel, S., Rubensdotter, L., 2012. Snow cornice dynamics as a control on plateau edge erosion in central Svalbard. Earth Surf. Process. Landf. 38 (5), 466–476.
Eckerstorfer, M., Christiansen, H.H., Rubensdotter, L., Vogel, S., 2013. The geomorphological effect of cornice fall avalanches in the Longyeardalen valley, Svalbard. Cryosphere 7 (5), 1361–1374.
Etzelmüller, B., Schuler, T., Isaksen, K., Christiansen, H., Farbrot, H., Benestad, R., 2011. Modeling the temperature evolution of Svalbard permafrost during the 20th and 21st century. Cryosphere 5 (1), 67–79.
Eyles, N., Kocsis, S., 1988. Sedimentology and clast fabric of subaerial debris flow facies in a glacially-influenced alluvial fan. Sediment. Geol. 59 (1), 15–28.
Fonstad, M.A., Dietrich, J.T., Courville, B.C., Jensen, J.L., Carbonneau, P.E., 2013. Topographic structure from motion: a new development in photogrammetric measurement. Earth Surf. Process. Landf. 38 (4), 421–430.

Førland, E.J., Hanssen-Bauer, I., 2003. Past and future climate variations in the Norwegian Arctic: overview and novel analyses. Polar Res. 22 (2), 113–124.
Førland, E., Hanssen-Bauer, I., Nordli, P., 1997. Climate statistics and longterm series of temperature and precipitation at Svalbard and Jan Mayen. Norwegian Meteorological Institude Report, 21/97.
Førland, E.J., Benestad, R., Hanssen-Bauer, I., Haugen, J.E., Skaugen, T.E., 2012. Temperature and precipitation development at Svalbard 1900–2100. Adv. Meteorol. 2011.
Frankel, K.L., Dolan, J.F., 2007. Characterizing arid region alluvial fan surface roughness with airborne laser swath mapping digital topographic data. J. Geophys. Res. 112 (F2), F02025.
Friend, D.A., Phillips, F.M., Campbell, S.W., Liu, T., Sharma, P., 2000. Evolution of desert colluvial boulder slopes. Geomorphology 36 (1), 19–45.
Frings, R.M., 2008. Downstream fining in large sand-bed rivers. Earth Sci. Rev. 87 (1), 39–60.
Gwinner, K., Hauber, E., Jaumann, R., Neukum, G., 2000. High-resolution, digital photogrammetric mapping: a tool for Earth science. EOS Trans. Am. Geophys. Union 81 (44), 513–520.
Hanssen-Bauer, I., Førland, E., 1998. Long-term trends in precipitation and temperature in the Norwegian Arctic: can they be explained by changes in atmospheric circulation patterns? Clim. Res. 10 (2), 143–153.
Harris, S.A., Gustafson, C.A., 1993. Debris flow characteristics in an area of continuous permafrost, St. Elias Range, Yukon Territory. Z. Geomorphol. 37, 41–56.
Harris, C., Lewkowicz, A.G., 2000. An analysis of the stability of thawing slopes, Ellesmere Island, Nunavut, Canada. Can. Geotech. J. 37 (2), 449–462.
Harris, S., McDermid, G., 1998. Frequency of debris flows on the Sheep Mountain fan, Kluane Lake, Yukon Territory. Z. Geomorphol. 42 (2), 159–175.
Harris, C., Arenson, L.U., Christiansen, H.H., Etzelmüller, B., Frauenfelder, R., Gruber, S., Haeberli, W., Hauck, C., Hölzle, M., Humlum, O., Isaksen, K., Kääb, A., Kern-Lütschg, M.A., Lehning, M., Matsuoka, N., Murton, J.B., Nötzli, J., Phillips, M., Ross, N., Seppälä, M., Springman, S.M., Mühll, D.V., 2009. Permafrost and climate in Europe: Monitoring and modelling thermal, geomorphological and geotechnical responses. Earth-Science Reviews. 92 (3), 117–171.
Harris, C., Kern-Luetschg, M., Christiansen, H.H., Smith, F., 2011. The role of interannual climate variability in controlling solifluction processes, Endalen, Svalbard. Permafr. Periglac. Process. 22 (3), 239–253.
Hartley, A.J., Mather, A.E., Jolley, E., Turner, P., 2005. Alluvial fans: geomorphology, sedimentology, dynamics. Geological Society London Special Publication, Ch. Climatic controls on alluvial-fan activity, Coastal Cordillera, northern Chile. pp. 95–115.
Hartley, A.J., Weissmann, G.S., Nichols, G.J., Warwick, G.L., 2010. Large distributive fluvial systems: characteristics, distribution, and controls on development. J. Sediment. Res. 80 (2), 167–183.
Harvey, A.M., 2010. Sediment cascades: an integrated approach. Local Buffers to the Sediment Cascade: Debris Cones and Alluvial Fans. John Wiley & Sons, Ltd., Ch., pp. 153–180.
Harvey, A., 2011. Dryland alluvial fans. Arid Zone Geomorphology: Process, Form and Change in Drylands Third edition. pp. 333–371.
Harvey, A.M., Mather, A.E., Stokes, M., 2005. Alluvial fans: geomorphology, sedimentology, dynamics — introduction. A review of alluvial-fan research. Geol. Soc. Lond., Spec. Publ. 251 (1), 1–7.
Hauber, E., Reiss, D., Ulrich, M., Preusker, F., Trauthan, F., Zanetti, M., Hiesinger, H., Jaumann, R., Johansson, L., Johnsson, A., O. M. C. E. J. H. M. S., 2011. Landscape evolution in Martian mid-latitude regions: insights from analogous periglacial landforms in Svalbard. Geol. Soc. Lond., Spec. Publ. 356 (1), 111–131.
Hauber, E., Platz, T., Reiss, D., Le Deit, L., Kleinhans, M.G., Marra, W.A., de Haas, T., Carbonneau, P., 2013. Asynchronous formation of Hesperian and Amazonian-aged deltas on Mars and implications for climate. J. Geophys. Res. Planets 118 (7), 1529–1544.
Hestnes, E., 1998. Slushflow hazard—where, why and when? 25 years of experience with slushflow consulting and research. Ann. Glaciol. 26, 370–376.
Humlum, O., Christiansen, H.H., Juliussen, H., 2007. Avalanche-derived rock glaciers in Svalbard. Permafr. Periglac. Process. 18 (1), 75–88.
Huscroft, C.A., Lipovsky, P., Bond, J.D., 2003. Permafrost and landslide activity: case studies from southwestern Yukon Territory. Yukon Geological Survey, pp. 107–119.
Ibbeken, H., Warnke, D.A., Diepenbroek, M., 1998. Granulometric study of the Hanaupah Fan, Death Valley, California. Earth Surf. Process. Landf. 23 (6), 481–492.
Isaksen, K., Mühll, D.V., Gubler, H., Kohl, T., Sollid, J.L., 2000. Ground surface-temperature reconstruction based on data from a deep borehole in permafrost at Janssonhaugen, Svalbard. Ann. Glaciol. 31 (1), 287–294.
Isaksen, K., Holmlund, P., Sollid, J.L., Harris, C., 2001. Three deep Alpine-permafrost boreholes in Svalbard and Scandinavia. Permafr. Periglac. Process. 12 (1), 13–25.
Isaksen, K., Sollid, J.L., Holmlund, P., Harris, C., 2007. Recent warming of mountain permafrost in Svalbard and Scandinavia. J. Geophys. Res. Earth Surf. (2003–2012) 112 (F2), F02S04.
Jahn, A., 1967. Some features of mass movement on Spitsbergen slopes. Geogr. Ann. Ser. A Phys. Geogr. 49, 213–225.
Jahn, A., 1976. Contemporaneous geomorphological processes in Longyeardalen, Vest-Spitsbergen (Svalbard). Biul. Peryglac. 26, 253–268.
Jamieson, J.B., Schweizer, J., 2000. Texture and strength changes of buried surface-hoar layers with implications for dry snow-slab avalanche release. J. Glaciol. 46 (152), 151–160.
Jaumann, R., Neukum, G., Behnke, T., Duxbury, T., Eichentopf, K., Flohrer, J., Gasselt, S., Giese, B., Gwinner, K., Hauber, E., Hoffmann, H., Hoffmeister, A., Köhler, U., Matz, K.-D., McCord, T., Mertens, V., Oberst, J., Pischel, R., Reiss, D., Ress, E., Roatsch, T., Saiger, P., Scholten, F., Schwarz, G., Stephan, K., Wählisch, M., 2007. The high-resolution stereo camera (HRSC) experiment on Mars Express: instrument aspects and experiment conduct from interplanetary cruise through the nominal mission. Planet. Space Sci. 55 (7), 928–952.
Jóhannesson, T., Arnalds, T., 2001. Accidents and economic damage due to snow avalanches and landslides in Iceland. Jökull 50, 81–94.
Johnsson, A., Reiss, D., Hauber, E., Zanetti, M., Hiesinger, H., Johansson, L., Olvmo, M., 2012. Periglacial mass-wasting landforms on Mars suggestive of transient liquid water in the recent past: insights from solifluction lobes on Svalbard. Icarus 218 (1), 489–505.
Jomelli, V., Bertran, P., 2001. Wet snow avalanche deposits in the French Alps: structure and sedimentology. Geogr. Ann. Ser. A Phys. Geogr. 83 (1–2), 15–28.
Jomelli, V., Francou, B., 2000. Comparing the characteristics of rockfall talus and snow avalanche landforms in an Alpine environment using a new methodological approach: Massif des Ecrins, French Alps. Geomorphology 35 (3), 181–192.
Kesel, R., Spicer, B., 1985. Geomorphologic relationships and ages of soils on alluvial fans in the Rio General valley, Costa Rica. Catena 12 (1), 149–166.
Kostaschuk, R., MacDonald, G., Putnam, P., 1986. Depositional process and alluvial fan-drainage basin morphometric relationships near Banff, Alberta, Canada. Earth Surf. Process. Landf. 11 (5), 471–484.
Kronholm, K., Vikhamar-Schuler, D., Jaedicke, C., Isaksen, K., Sorteberg, A., Kristensen, K., 2006. Forecasting snow avalanche days from meteorological data using classification trees; Grasdalen, Western Norway. Proceedings of the International Snow Science Workshop, Telluride, Colorado, pp. 1–6.
Krzyszkowski, D., Zieliński, T., 2002. The Pleistocene end moraine fans: controls on their sedimentation and location. Sediment. Geol. 149 (1), 73–92.
Lafortune, V., Filion, L., Hétu, B., 2006. Impacts of Holocene climatic variations on alluvial fan activity below snowpatches in subarctic Québec. Geomorphology 76 (3), 375–391.
Larsson, S., 1982. Geomorphological effects on the slopes of Longyear valley, Spitsbergen, after a heavy rainstorm in July 1972. Geogr. Ann. Ser. A Phys. Geogr. 64, 105–125.
Latham, J., Montagne, J., 1970. The possible importance of electrical forces in the development of snow cornices. J. Glaciol. 9, 375–384.
Laute, K., Beylich, A.A., 2014. Morphometric and meteorological controls on recent snow avalanche distribution and activity at hillslopes in steep mountain valleys in western Norway. Geomorphology 218, 16–34.
Legget, R.F., Brown, R.E., Johnston, G.H., 1966. Alluvial fan formation near Aklavik, Northwest Territories, Canada. Geol. Soc. Am. Bull. 77 (1), 15–30.
Lewkowicz, A.G., Harris, C., 2005. Morphology and geotechnique of active-layer detachment failures in discontinuous and continuous permafrost, northern Canada. Geomorphology 69 (1), 275–297.
Liestøl, O., 1976. Pingos, springs and permafrost in Spitsbergen. Norsk Polarinstitutt Årbok 1975, pp. 7–29.
Lønne, I., Nemec, W., 2004. High-arctic fan delta recording deglaciation and environment disequilibrium. Sedimentology 51 (3), 553–589.
Lorenz, R.D., Lopes, R.M., Paganelli, F., Lunine, J.I., Kirk, R.L., Mitchell, K.L., Soderblom, L.A., Stofan, E.R., Ori, G., Myers, M., et al., 2008. Fluvial channels on Titan: initial Cassini RADAR observations. Planet. Space Sci. 56 (8), 1132–1144.
Luckman, B., 1977. The geomorphic activity of snow avalanches. Geogr. Ann. Ser. A Phys. Geogr. 31–48.
Luckman, B., 1992. Debris flows and snow avalanche landforms in the Lairig Ghru, Cairngorm Mountains, Scotland. Geogr. Ann. Ser. A Phys. Geogr. 74, 109–121.
Major, H., Nagy, J., 1972. Geology of the Adventdalen map area. Nor. Polarinst. Skr. 138.
Mangerud, J., Bolstad, M., Elgersma, A., Helliksen, D., Landvik, J.Y., Lønne, I., Lycke, A.K., Salvigsen, O., Sandahl, T., Svendsen, J.I., 1992. The last glacial maximum on Spitsbergen, Svalbard. Quat. Res. 38 (1), 1–31.
Matmon, A., Nichols, K., Finkel, R., 2006. Isotopic insights into smoothening of abandoned fan surfaces, Southern California. Quat. Res. 66 (1), 109–118.
Matsuoka, N., 1991. A model of the rate of frost shattering: application to field data from Japan, Svalbard and Antarctica. Permafr. Periglac. Process. 2 (4), 271–281.
Matsuoka, N., 2001. Solifluction rates, processes and landforms: a global review. Earth Sci. Rev. 55 (1), 107–134.
Matsuoka, N., Hirakawa, K., 2000. Solifluction resulting from one-sided and two-sided freezing: field data from Svalbard. Polar Geosci. 13, 187–201.
Mercier, D., Étienne, S., Sellier, D., André, M.-F., 2009. Paraglacial gullying of sediment-mantled slopes: a case study of Colletthøgda, Kongsfjorden area, West Spitsbergen (Svalbard). Earth Surf. Process. Landf. 34 (13), 1772–1789.
Moscariello, A., Marchi, L., Maraga, F., Mortara, G., 2002. Alluvial fans in the Italian Alps: sedimentary facies and processes. Flood and Megaflood Processes and Deposits: Recent and Ancient Examples (Special Publication 32 of the IAS) 32 pp. 141–166.
Nater, P., Arenson, L.U., Springman, S.M., 2008. Choosing geotechnical parameters for slope stability assessments in Alpine permafrost soils. Ninth International Conference on Permafrost vol. 29. University of Alaska Fairbanks, pp. 1261–1266.
Nemec, W., Postma, G., 1993. Alluvial sedimentation. Quaternary alluvial fans in southwestern Crete: sedimentation processes and geomorphic, evolution. Blackwell Publishing Ltd., Oxford, UK, Ch, pp. 235–276.
Nesje, A., Bakke, J., Dahl, S.O., Lie, Ø., Bøe, A.-G., 2007. A continuous, high-resolution 8500-yr snow-avalanche record from western Norway. The Holocene 17 (2), 269–277.
Neukum, G., the HRSC-Team, 2001. The Airborne HRSC-AX cameras: evaluation of the technical concept and presentation of application results after one year of operations. Photogrammetric Week vol. 1, pp. 117–130.
Nicholas, A., Clarke, L., Quine, T., 2009. A numerical modelling and experimental study of flow width dynamics on alluvial fans. Earth Surf. Process. Landf. 34 (15), 1985–1993.
Nyberg, R., 1989. Observations of slushflows and their geomorphological effects in the Swedish mountain area. Geogr. Ann. A 71 (3–4), 185–198.
Owen, L.A., Sharma, M.C., 1998. Rates and magnitudes of paraglacial fan formation in the Garhwal Himalaya: implications for landscape evolution. Geomorphology 26 (1), 171–184.
Parker, J.R., 1967. The Jurassic and Cretaceous sequence in Spitsbergen. Geol. Mag. 104 (5), 487–505.
Pavlova, I., Jomelli, V., Brunstein, D., Grancher, D., Martin, E., Déqué, M., 2014. Debris flow activity related to recent climate conditions in the French Alps: a regional investigation. Geomorphology 219, 248–259.

Rachlewicz, G., 2010. Paraglacial modifications of glacial sediments over millennial to decadal time-scales in the high Arctic (Billefjorden, central Spitsbergen, Svalbard). Quaest. Geographicae 29 (3), 59–67.
Rapp, A., 1960. Talus slopes and mountain walls at Tempelfjorden, Spitsbergen: a geomorphological study of the denudation of slopes in an arctic locality. Nor. Polarinst. Skr. 119, 1–96.
Rapp, A., 1985. Extreme rainfall and rapid snowmelt as causes of mass movements in high latitude mountains. Field and Theory, Lectures Geocryologypp. 36–56.
Rapp, A., 1986. Slope processes in high latitude mountains. Prog. Phys. Geogr. 10 (1), 53–68.
Rebetez, M., Lugon, R., Baeriswyl, P.-A., 1997. Climatic change and debris flows in high mountain regions: the case study of the Ritigraben torrent (Swiss Alps). Clim. Chang. 36 (3–4), 371–389.
Reiss, D., Hauber, E., Hiesinger, H., Jaumann, R., Trauthan, F., Preusker, F., Zanetti, M., Ulrich, M., Johnsson, A., Johansson, L., et al., 2011. Terrestrial gullies and debris-flow tracks on Svalbard as planetary analogs for Mars. Geol. Soc. Am. Spec. Pap. 483, 165–175.
Rist, A., 2008. Hydrothermal Processes Within the Active Layer Above Alpine Permafrost in Steep Scree Slopes and Their Influence on Slope Stability. Ph.D. Thesis. Geograph. Inst. der Univ. Zürich.
Ritter, J.B., Miller, J.R., Enzel, Y., Wells, S.G., 1995. Reconciling the roles of tectonism and climate in Quaternary alluvial fan evolution. Geology 23 (3), 245–248.
Romanovsky, V., Drozdov, D., Oberman, N., Malkova, G., Kholodov, A., Marchenko, S., Moskalenko, N., Sergeev, D., Ukraintseva, N., Abramov, A., et al., 2010. Thermal state of permafrost in Russia. Permafr. Periglac. Process. 21 (2), 136–155.
Roof, S., Werner, A., 2011. Indirect growth curves remain the best choice for lichenometry: evidence from directly measured growth rates from Svalbard. Arct. Antarct. Alp. Res. 43 (4), 621–631.
Rozema, J., Boelen, P., Solheim, B., Zielke, M., Buskens, A., Doorenbosch, M., Fijn, R., Herder, J., Callaghan, T., Björn, L.O., et al., 2006. Stratospheric ozone depletion: high arctic tundra plant growth on Svalbard is not affected by enhanced UV–B after 7 years of UV–B supplementation in the field. Plant Ecol. 182 (1–2), 121–135.
Ryder, J., 1971. The stratigraphy and morphology of para-glacial alluvial fans in south-central British Columbia. Can. J. Earth Sci. 8 (2), 279–298.
Saito, K., Oguchi, T., 2005. Slope of alluvial fans in humid regions of Japan, Taiwan and the Philippines. Geomorphology 70 (1), 147–162.
Sattler, K., Keiler, M., Zischg, A., Schrott, L., 2011. On the connection between debris flow activity and permafrost degradation: a case study from the Schnalstal, South Tyrolean Alps, Italy. Permafr. Periglac. Process. 22 (3), 254–265.
Schoeneich, P., Dall'Amico, M., Deline, P., Zischg, A., 2011. Hazards related to permafrost and to permafrost degradation. PermaNET Project, Report 6.2. ISBN: 978-2-903095-59-8 (On-line publication).
Siewert, M.B., Krautblatter, M., Christiansen, H.H., Eckerstorfer, M., 2012. Arctic rockwall retreat rates estimated using laboratory-calibrated ERT measurements of talus cones in Longyeardalen, Svalbard. Earth Surf. Process. Landf. 37 (14), 1542–1555.
Smith, S., Romanovsky, V., Lewkowicz, A., Burn, C., Allard, M., Clow, G., Yoshikawa, K., Throop, J., 2010. Thermal state of permafrost in North America: a contribution to the International Polar Year. Permafr. Periglac. Process. 21 (2), 117–135.
Sollid, J., Holmlund, P., Isaksen, K., Harris, C., 2000. Deep permafrost boreholes in western Svalbard, northern Sweden and southern Norway. Nor. Geogr. Tidsskr. 54 (4), 186–191.
Sørbel, L., Tolgensbakk, J., 2002. Ice-wedge polygons and solifluction in the Adventdalen area, Spitsbergen, Svalbard. Nor. Geogr. Tidsskr. 56 (2), 62–66.
Sørbel, L., Tolgensbakk, J., Hagen, J., Hogvard, K., 2011. Geomorphological and quaternary geological map of Svalbard, 1:100,000, C9G Adventdalen. Norsk Polar Institutt Temakart 31/32.
Svendsen, J.I., Mangerud, J., 1997. Holocene glacial and climatic variations on Spitsbergen, Svalbard. The Holocene 7 (1), 45–57.
Szpikowski, J., Szpikowska, G., Zwoliński, Z., Rachlewicz, G., Kostrzewski, A., Marciniak, M., Dragon, K., 2014. Character and rate of denudation in a High Arctic glacierized catchment (Ebbaelva, Central Spitsbergen). Geomorphology 218, 52–62.
Thiedig, v.F., Kresling, A., 1973. Meteorologische und geologische Bedingungen bei der Entstehung von Muren im Juli 1972 auf Spitzbergen. Polarforschung 43 (1/2), 40–49.
Van Dijk, M., Kleinhans, M.G., Postma, G., Kraal, E., 2012. Contrasting morphodynamics in alluvial fans and fan deltas: effect of the downstream boundary. Sedimentology 59 (7), 2125–2145.
Van Vliet-Lanoë, B., 1998. Frost and soils: implications for paleosols, paleoclimates and stratigraphy. Catena 34 (1), 157–183.
Ventra, D., Diaz, G.C., de Boer, P.l., 2013. Colluvial sedimentation in a hyperarid setting (Atacama Desert, northern Chile): geomorphic controls and stratigraphic facies variability. Sedimentology 60 (5), 1257–1290.
Vogel, S., Eckerstorfer, M., Christiansen, H., 2012. Cornice dynamics and meteorological control at Gruvefjellet, Central Svalbard. Cryosphere 6 (1), 157–171.
Webb, J., Fielding, C.R., 1999. Debris flow and sheetflood fans of the northern Prince Charles Mountains, East Antarctica. In: Miller, A.J., Gupta, A. (Eds.), Varieties of Fluvial form. Wiley, pp. 317–341.
Weissmann, G., Hartley, A., Nichols, G., Scuderi, L., Olson, M., Buehler, H., Banteah, R., 2010. Fluvial form in modern continental sedimentary basins: distributive fluvial systems. Geology 38 (1), 39–42.
Wells, S.G., McFadden, L.D., Dohrenwend, J.C., 1987. Influence of late Quaternary climatic changes on geomorphic and pedogenic processes on a desert piedmont, Eastern Mojave Desert, California. Quat. Res. 27 (2), 130–146.
Werner, A., 1990. Lichen growth rates for the northwest coast of Spitsbergen, Svalbard. Arct. Alp. Res. 22 (2), 129–140.
Whipple, K.X., Dunne, T., 1992. The influence of debris-flow rheology on fan morphology, Owens Valley, California. Geol. Soc. Am. Bull. 104 (7), 887–900.
Zimmermann, M., Haeberli, W., 1993. Climatic change and debris flow activity in high-mountain areas—a case study in the Swiss Alps. Catena Suppl. 22, 59–72.